REPORT NO. FAA-RD-79-97
FAA-79-22

AN INVESTIGATION OF LASER LIGHTING SYSTEMS TO ASSIST AIRCRAFT LANDING

D.C. Burnham
J.F. Fantasia

U.S. DEPARTMENT OF TRANSPORTATION
RESEARCH AND SPECIAL PROGRAMS ADMINISTRATION
Transportation Systems Center
Cambridge MA 02142

OCTOBER 1979

FINAL REPORT

DOCUMENT IS AVAILABLE TO THE PUBLIC THROUGH THE NATIONAL TECHNICAL INFORMATION SERVICE, SPRINGFIELD, VIRGINIA 22161

Prepared for

U.S. DEPARTMENT OF TRANSPORTATION
FEDERAL AVIATION ADMINISTRATION
Systems Research and Development Service
Washington DC 20591

Technical Report Documentation Page

1. Report No.	2. Government Accession No.	3. Recipient's Catalog No.
FAA-RD-79-97		

4. Title and Subtitle	5. Report Date
AN INVESTIGATION OF LASER LIGHTING SYSTEMS TO ASSIST AIRCRAFT LANDING	October 1979
	6. Performing Organization Code
7. Author(s) D.C. Burnham, J.F. Fantasia	8. Performing Organization Report No. DOT-TSC-FAA-79-22
9. Performing Organization Name and Address U.S. Department of Transportation Research and Special Programs Administration Transportation Systems Center Cambridge MA 02142	10. Work Unit No. (TRAIS) FA973/R9141
	11. Contract or Grant No.
	13. Type of Report and Period Covered Final Report Oct 1978-Sep 1979
12. Sponsoring Agency Name and Address U.S. Department of Transportation Federal Aviation Administration Systems Research and Development Service Washington DC 20591	14. Sponsoring Agency Code

15. Supplementary Notes

16. Abstract

A model for the visual detectability of narrow light beams was developed and used to evaluate the system performance of two laser lighting system configurations: (1) a laser VASI and (2) a crossed beam glide path indicator. Laboratory experiments confirmed the validity of the model. Using a criterion taken from the Federal Standard for laser safety, the potential hazards of each of the system concepts were evaluated. The following results were obtained for readily available laser power levels: Neither system will work during bright daylight. The laser VASI can be seen at night at the middle marker for visual ranges greater than 5000 ft. The crossed beam system can be seen at night at the middle marker for visual ranges greater than 700 ft.

17. Key Words	18. Distribution Statement
Laser Landing System Illumination	DOCUMENT IS AVAILABLE TO THE PUBLIC THROUGH THE NATIONAL TECHNICAL INFORMATION SERVICE, SPRINGFIELD, VIRGINIA 22161

19. Security Classif. (of this report)	20. Security Classif. (of this page)	21. No. of Pages	22. Price
Unclassified	Unclassified	64	

Form DOT F 1700.7 (8-72) Reproduction of completed page authorized

PREFACE

Major airports throughout the world are equipped with specialized lighting systems that provide visual guidance to pilots for all aircraft operations. Lights provide pilots with basic decision-making cues during final approach to an airport runway. To be effective they must be visible well in advance of the decision height. Visibility of a light depends on brightness, distance, and the atmosphere prevailing at the particular time. Another important factor is contrast; i.e., the difference between a light and its surroundings. Contrast can be affected by variations in brightness and/or color of the light. Lasers are ideally suited as visual guidance lights because they offer very high brightness and are monochromatic. However, these same characteristics can be hazardous and must be evaluated for safety. The goal of this report is to determine if lasers can be safely used to improve final approach guidance to a runway or helicopter pad so that landings can be made reliably under minimum visibility conditions.

We wish to thank Robert Bostrom and Robert James, of the Bureau of Radiological Health, for their suggestions and comments on laser safety. We would also like to thank James Hallock and William Wood for their suggestions and comments on the final draft of the report.

METRIC CONVERSION FACTORS

Approximate Conversions to Metric Measures

Symbol	When You Know	Multiply by	To Find	Symbol
		LENGTH		
in	inches	2.5	centimeters	cm
ft	feet	30	centimeters	cm
yd	yards	0.9	meters	m
mi	miles	1.6	kilometers	km
		AREA		
in^2	square inches	6.5	square centimeters	cm^2
ft^2	square feet	0.09	square meters	m^2
yd^2	square yards	0.8	square meters	m^2
mi^2	square miles	2.6	square kilometers	km^2
	acres	0.4	hectares	ha
		MASS (weight)		
oz	ounces	28	grams	g
lb	pounds	0.45	kilograms	kg
	short tons (2000 lb)	0.9	tonnes	t
		VOLUME		
tsp	teaspoons	5	milliliters	ml
Tbsp	tablespoons	15	milliliters	ml
fl oz	fluid ounces	30	milliliters	ml
c	cups	0.24	liters	l
pt	pints	0.47	liters	l
qt	quarts	0.95	liters	l
gal	gallons	3.8	liters	l
ft^3	cubic feet	0.03	cubic meters	m^3
yd^3	cubic yards	0.76	cubic meters	m^3
		TEMPERATURE (exact)		
°F	Fahrenheit temperature	5/9 (after subtracting 32)	Celsius temperature	°C

Approximate Conversions from Metric Measures

Symbol	When You Know	Multiply by	To Find	Symbol
		LENGTH		
mm	millimeters	0.04	inches	in
cm	centimeters	0.4	inches	in
m	meters	3.3	feet	ft
m	meters	1.1	yards	yd
km	kilometers	0.6	miles	mi
		AREA		
cm^2	square centimeters	0.16	square inches	in^2
m^2	square meters	1.2	square yards	yd^2
km^2	square kilometers	0.4	square miles	mi^2
ha	hectares (10,000 m^2)	2.5	acres	
		MASS (weight)		
g	grams	0.035	ounces	oz
kg	kilograms	2.2	pounds	lb
t	tonnes (1000 kg)	1.1	short tons	
		VOLUME		
ml	milliliters	0.03	fluid ounces	fl oz
l	liters	2.1	pints	pt
l	liters	1.06	quarts	qt
l	liters	0.26	gallons	gal
m^3	cubic meters	35	cubic feet	ft^3
m^3	cubic meters	1.3	cubic yards	yd^3
		TEMPERATURE (exact)		
°C	Celsius temperature	9/5 (then add 32)	Fahrenheit temperature	°F

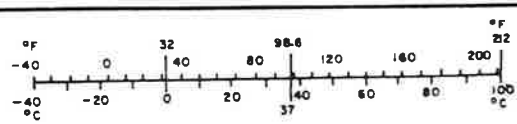

TABLE OF CONTENTS

LIST OF ILLUSTRATIONS

LIST OF TABLES

1. INTRODUCTION

The recent issuance of a US patent [1] for the Russian Glissada laser-based aircraft landing system has stimulated a new look at the feasibility of using lasers to improve the approach lighting at airports. Present lighting can be inadequate under conditions of a ragged ceiling near the minimum decision height. In particular, the transition from an instrument landing system to visual acquisition of the ground could be made more reliable by improved lighting.

The question of laser-based aircraft landing systems was studied five years ago for the FAA by Viezee, Oblanas, and Glaser [2]. Their work formed the starting point for this report. The fundamental question that they addressed was how far a laser beam could penetrate a low-visibility atmosphere without exposing a pilot to an eye hazard. The Russian Glissada system raises two additional questions. The first is how well a pilot can see a narrow light beam via scattered rather than direct light. The second is whether a high-power infrared laser beam can be used to burn a hole through a fog so that a visible light beam can propagate with little loss in intensity. To answer these questions a study and an experimental measurements program were performed.

The program began with an analysis of laser beam propagation. Beam propagation was examined as a visual phenomenon and was therefore directly related to atmospheric attenuation and the dynamic visual response of the eye. In order to determine the detectability of light scattered from a narrow light beam, a theoretical model was developed. This new model included the effects of the geometry and luminance of the source, luminance of the background, and some of the optical characteristics of the human eye.

Measurements of simulated atmospheric scattering were performed in the laboratory to test the validity of the theoretical

model. Once satisfied that the model was valid, calculations were made of several system configurations to determine feasibility.

Calculations were made to determine if it was feasible to use a laser to clear a path through fog along the flight path such that a visible laser beam could propagate along the cleared path and provide a guiding beam for aircraft on approach.

The eye hazard posed to a pilot by a visible laser beam guidance system was analyzed by considering each system configuration and the type of viewing. Use was made of the recent federal standard for laser products.

2. THEORY OF LASER BEAMS AS VISUAL AIDS

Under conditions of minimum visibility, the present approach lighting system is used in the following way. A pilot's first visual contact with the ground is the approach lights which must be visible when he reaches his decision height. The pilot follows the approach lights down until he can see the runway edge lights at some time before he flares for landing.

There are three difficulties associated with the present system: First, the approach lights do not provide guidance to the pilot with regard to his altitude (i.e., with respect to the glideslope) and, thus, he must continue to monitor his instruments. Second, under conditions of a ragged ceiling the pilot may not acquire the approach lights as soon as desired and may lose them after they are acquired. Third, the large number of approach lights may present problems with the pilot's ability to see any particular light because of the background glow produced by the scattered light.

The following sections will summarize and expand on the results obtained by the Viezee report. Also, a theory for viewing a narrow light beam via scattered light is developed, and the amount of laser power required to burn a hole through a fog is calculated.

2.1 BEAM PROPAGATION

Apart from the coherence effects which produce laser speckle, the propagation of laser and conventional light beams is affected similarly by atmospheric attenuation and scattering. A uniform extinction coefficient σ governs the beam attenuation over a distance Z by the equation

$$E_{(Z)} = E_o(Z)\, e^{-\sigma Z}, \qquad (1)$$

where $E_o(Z)$ is the illuminance in the beam without attenuation. For a diverging source of luminous intensity I, $E_o(Z)$ is given by

I/z^2. As discussed by the Viezee report, the extinction coefficient can be related to the Runway Visual Range (RVR), which is the distance the runway lights can be seen. The value of σ giving a specified RVR depends upon the background illuminance; e.g., skylight and the brightness of the runway lights. Table 1 shows values of σ for various values of RVR for runway lights set for maximum brightness of 10,000 cd (L.S.5)[3]. These numbers will be used in subsequent calculations.

TABLE 1. DAY AND NIGHT EXTINCTION COEFFICIENTS FOR VARIOUS VALUES OF RUNWAY VISUAL RANGES [L.S.5]

RVR (FT)	σ DAY$^{(m-1)}$	σ NIGHT$^{(m-1)}$
150	2.06×10^{-1}	3.42×10^{-1}
300	4.18×10^{-2}	1.56×10^{-1}
700	2.97×10^{-2}	5.89×10^{-2}
1,200	1.44×10^{-2}	3.09×10^{-2}
2,400	5.30×10^{-3}	1.38×10^{-2}
5,000	1.90×10^{-3}	5.66×10^{-3}
10,000	9.52×10^{-4}	2.38×10^{-3}
25,000	3.81×10^{-4}	7.10×10^{-4}
50,000	1.90×10^{-4}	2.64×10^{-4}

2.2 DYNAMIC RANGE OF THE EYE

One can define a dynamic range for the eye as the ratio of the maximum eye-safe incident intensity to the minimum detectable intensity. For a 10-second exposure the maximum eye-safe irradiance is 10 W/m^2 (see Section 6). The illuminance threshold of the eye for a point source is usually taken as 7.7×10^{-7} lm/m^2 at night and a factor of 500 times larger for daytime. This threshold can be related to a radiometric threshold irradiance by means of the eye's spectral luminous efficiency which has the peak value 673 lm/W at a wavelength λ of 555 nm. The eye's irradiance threshold becomes 1.14×10^{-9} W/m^2 for λ = 555 nm at night.

The dynamic range of the eye then becomes 101 dB at night and 74 dB during the day. Existing lighting systems make use of a significant fraction of this dynamic range. For example, the illuminance of the runway lights at L.S.5 is 1 lm/m^2 at 100 m distance. This value is 61 dB above the night detection threshold and 34 dB above the day threshold.

Suppose we increase the illuminance at 100 m to the eye-safe limit. How much will the RVR increase if it is initially 100 m? Since the dominant range dependence of equation (1) is in the exponent, the new RVR is simply the original RVR times the ratio of the dB dynamic range, which equals the new dB attenuation, to the original dB attenuation: $\log A_1/\log A_2 = \sigma z_1/\sigma z_2$. We see from Table 2 that the increase in range is relatively small as found by the Viezee data for the use of laser sources. Contrary to the Viezee statement, the potential improvement is actually slightly better during the day.

TABLE 2. POTENTIAL RVR IMPROVEMENT

	DYNAMIC RANGE	100 m ATTENUATION	RANGE INCREASE
Night	101 dB	61 dB	x 1.66
Day	74 dB	34 dB	x 2.18

2.3 BACKGROUND GLOW

Under some conditions, the light scattered from the light beam can raise the background luminance and thereby increase the detection threshold for a point source. This effect may be observed in viewing the approach lights, which appear as a glow in the sky before they can be perceived directly.

Let us calculate the magnitude of this effect; namely, how much a light of flux F can be attenuated before the multiply-scattered light becomes a glow or a background luminance B_o, which limits the direct view of the light.

We assume that the multiply-scattered light spreads out isotropically to give an illuminance at Range R of

$$E=F/4\ \pi\ R^2 \tag{2}$$

(assuming σ R>>1 so that most of the light is scattered). Further, let us assume that Lambert's law describes the luminance B at the surface of a sphere of radius R:

$$B = E \cos \alpha/\pi\ , \tag{3}$$

where α is the angle with respect to the normal to the sphere. The background luminance B_o looking toward the source becomes

$$B_o = F/4\pi^2R^2\ . \tag{4}$$

For N similar sources this equation must be multiplied by N. It would be very complicated and tedious to derive a more accurate model than this crude approach. The illuminance produced by the direct beam from the source at Range R is

$$E = F\ e^{-\sigma R}/R^2\ \Delta\Omega\ , \tag{5}$$

where $\Delta\Omega$ is the solid angle of the beam emitted by the source. (In the near field $R^2\Delta\Omega$ should be replaced by the actual area of the beam.)

Using daytime conditions when the point source threshold illuminance E_t is roughly proportional to the background luminance B_o, we obtain from reference 4:

$$\log E_t - \log B_o = -7.3\ . \tag{6}$$

We take the logarithms of equations 4 and 5:

$$\log E_t = -\sigma R_t/2.30 - 2 \log R_t - \log \Delta\Omega \tag{7}$$

and

$$\log B_o = -2 \log R_t - \log 4\pi^2 + \log N\ . \tag{8}$$

We have defined R_t as the range where the direct beam illuminance E is equal to detection threshold E_t. These equations can be combined to give the attenuation exponent dB at this range:

$$\sigma R_t / 0.230 = 73 + 10 \text{ Log } (4\pi^2/\Delta\Omega) - 10 \text{ Log } N . \qquad (9)$$

This equation describes how much attenuation is needed to have the detection limit set by the scattered light. Here is the physical explanation for these terms: The 73 represents the contrast and angular resolution of the eye for point sources. The log $(4\pi^2/\Delta\Omega)$ represents the directivity of the initial beam. The log N represents the interference of multiple sources. Let us now consider two cases:

1) A helium-neon (He-Ne) laser beam with 0.5 mrad divergence. For $\Delta\Omega = 1.9 \times 10^{-7}$ sr, we have an attenuation exponent $\sigma R/0.230 = 156$ dB. Background glow detection limitation can never arise in this case since the allowable attenuation is much greater than the dynamic range of the eye.

2) Landing lights with 20° x 30° beams, N = 40. Here we have $\sigma R/0.230 = 72$ dB of allowed attenuation. Thus it may be possible for the sky glow of the landing lights to obscure their own visibility within the dynamic range of the eye. [Note: At night, when equation (6) no longer applies, the allowed attenuation will decrease because E_t saturates at low values of B_o (e.g., below $B_o = 1.0$ cd/m^2/sr).]

3. LUMINANCE OF A NARROW LIGHT BEAM

A scattering medium is characterized by the volume scattering function $\beta'(\phi)$ (units: lumens scattered into unit solid angle per unit volume per lumen per unit area) [5]. The integral of $\beta'(\phi)$ gives the scattering coefficient b:

$$b = 2\pi \int_0^{\pi} \beta'(\phi) \sin \phi \, d\phi \tag{10}$$

In the absence of absorption, the light beam attenuates with distance Z as e^{-bZ}.

The coordinate system for calculating the scattering is shown in Figure 1. The beam shines down the Z axis. The observation axis (in the g direction) is inclined at an angle ϕ with respect to the beam axis. The luminance B of the beam in the observation direction is obtained by integrating the scattered light flux from a small cross-sectional area dS into a small solid angle $d\Omega$:

$$dF = d\Omega dS \int \beta'(\phi) \, E(g) \, dg, \tag{11}$$

where E(g) is the illuminance of the beam as a function of the g coordinate in the direction of observation. Assume a cylindrically symmetric beam illuminance E(r'), where $r'^2 = x'^2 + y'^2$. The distance of the observation spot from the middle of the beam is given by y'. The x' coordinate is related to the g coordinate by $x' = g \sin \phi$. The integral in equation (3) then becomes

$$B = \frac{\beta'(\phi)}{\sin \phi} \int E \left[(x'^2 + y'^2)^{1/2} \right] dx' \quad , \tag{12}$$

where we have also used the relationship $B = dF/dS d\Omega$. Now make the simplifying assumption of uniform illuminance E inside radius r and zero intensity outside. The illuminance E is related to the total beam flux F by $F = \pi r^2 E$.

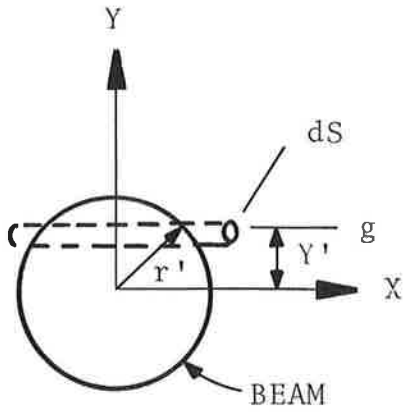

a) VIEW ALONG BEAM

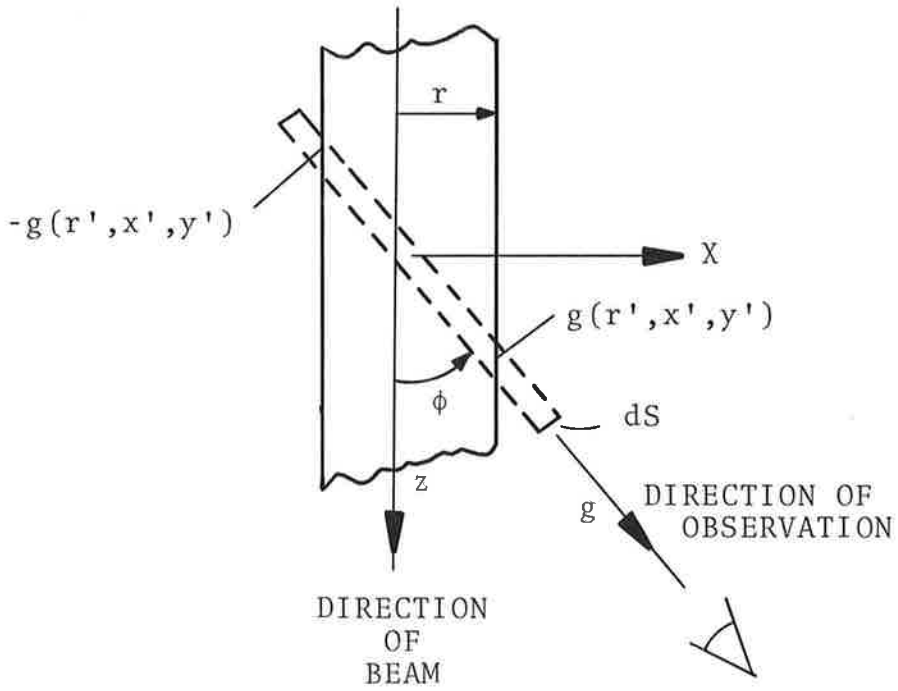

b) VIEW PERPENDICULAR TO BEAM

FIGURE 1. SCATTERING COORDINATE SYSTEM

The luminance becomes

$$B = \frac{F\beta'(\phi)}{\pi \sin\phi} \quad \frac{2(r^2-y'^2)^{1/2}}{r^2} \quad . \tag{13}$$

The peak luminance at the center of the beam is (y'=0):

$$B = \frac{2F\beta'(\phi)}{\pi r \sin \phi} \quad . \tag{14}$$

In many cases the angular width of the beam will be too small for the eye to resolve. In this case one can integrate the brightness across the beam y' to obtain the effective line intensity:

$$B = \frac{F\beta'(\phi)}{\sin \phi} \quad . \tag{15}$$

In order to evaluate the effective line intensity we need to have a model for $\beta'(\phi)$ for the atmosphere. We note that for a given type of scatterers, $\beta'(\phi)$ is proportional to b. Thus our model will give the ratio $\beta'(\phi)/b = \beta(\phi)$, which would be $1/4\pi$ for uniform scattering with respect to the scattering angle. We use data from Middleton [6] shown in Table 3.

TABLE 3. VOLUME SCATTERING FUNCTIONS

ϕ	$\beta'(\phi)$	b	$\beta(\phi)$
10°	7×10^{-4} m^{-1}	32×10^{-5} m^{-1}	2.2
45°	1.5×10^{-4}	32×10^{-5}	0.47

A model of the eye is required in order to determine the detectability of the light scattered from a narrow light beam. The model we adopt is developed in Appendix A and the final results are shown in Figures 2 and 3. Measurements by Lamar [7] have shown that the eye is sensitive to the contrast at the edge of a line. If the angular line width W is greater than a limiting angle $\Delta\theta$, the eye responds only to two bands of width, $\Delta\theta/2$ on each edge of the line. If the line width is less than $\Delta\theta$, then the eye responds

to the line luminance multiplied by the angular line width. Figure 2 shows the variation of $\Delta\theta$ with background luminance. Figure 3 shows the variation in the threshold product of luminance, B_t, and effective width, W_{eff}, as a function of background luminance, B_o, and the angular length L of the line. (Note: $B_o=10^4$ cd/m^2 for daytime and 10^{-2} cd/m^2 for night.) The dependence upon length L is relatively small as long as L is greater than the limiting value $\Delta\theta$.

We can now write expressions for the response product, $W_{eff}B$, for the two cases. For a beam at range R this product becomes

$$W_{eff}B = \frac{F\beta'(\phi)}{R \sin\phi} \quad , \tag{16}$$

for $2r<R\Delta\theta$. For the case of $2r>R\Delta\theta$, we make the approximation that the luminance at the edge of the beam is given by assigning a uniform luminance, B/2r. The response product then becomes

$$W_{eff}B = \frac{F\beta'(\phi)}{2r \sin\phi}\,\Delta\theta \quad . \tag{17}$$

The coordinate system is shown in Figure 4. We now properly include beam attenuation by means of the extinction coefficient σ and the initial beam flux F_o. Equations (16) and (17) become, respectively

$$W_{eff}B = \frac{\beta'(\phi)}{a} F_o e^{-\sigma(z+R)} \qquad [2r<R\Delta\theta] \tag{18}$$

and

$$W_{eff}B = \frac{R\Delta\theta\beta'(\phi)}{2ra} F_o e^{-\sigma(z+R)} \quad [2r>R\Delta\theta]. \tag{19}$$

Let us now consider where the beam is most easily detected for a fixed observer. As the scattering angle ϕ decreases (i.e., as R increases), $\beta'(\phi)$ increases until it approaches the value $\beta'(0)$ for small scattering angles. Since z+R is constant for small scattering angles, the attenuation terms do not affect the beam detection for small values of a/R. We are then left with a signal that increases with range R until $R = 2r/\Delta\theta$ and then becomes independent of range. Thus, the beam is most easily detected near its origin.

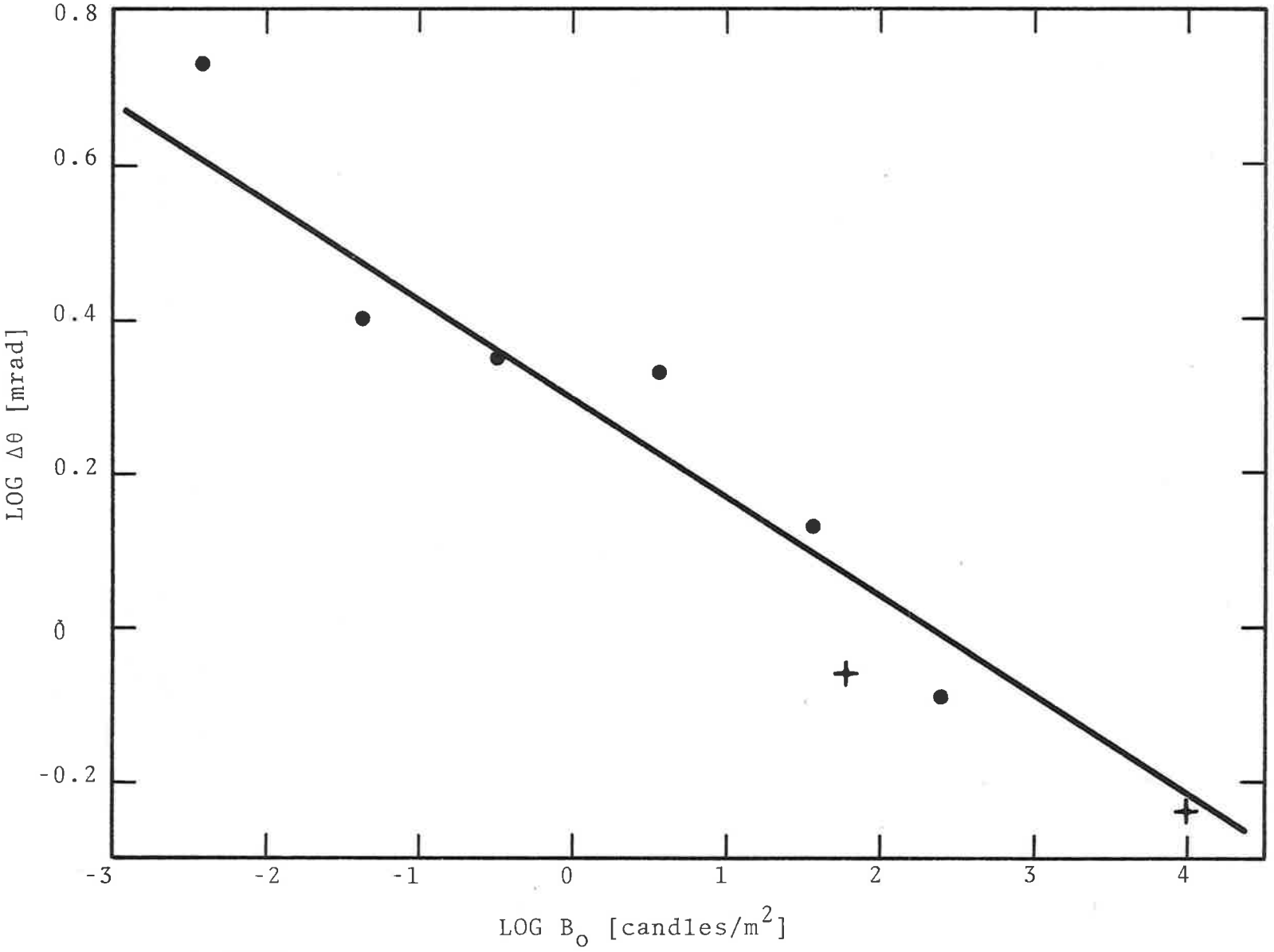

FIGURE 2. VARIATION OF VISUAL ANGLE AS A FUNCTION OF BACKGROUND LUMINANCE

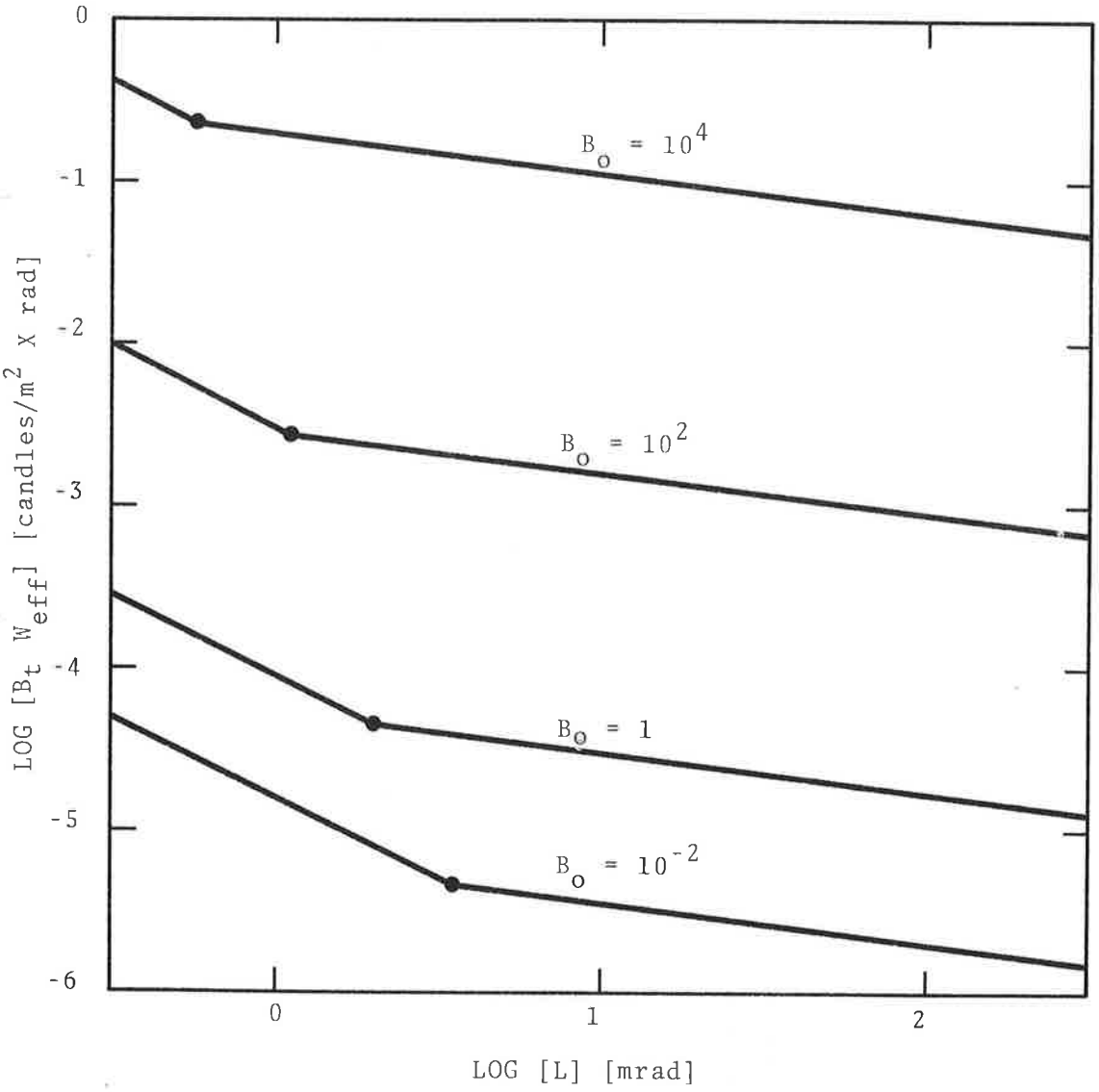

FIGURE 3. VARIATION OF THE THRESHOLD PRODUCT B_t W_{eff} AS A FUNCTION OF BACKGROUND LUMINANCE B_o AND BEAM ANGULAR LENGTH L

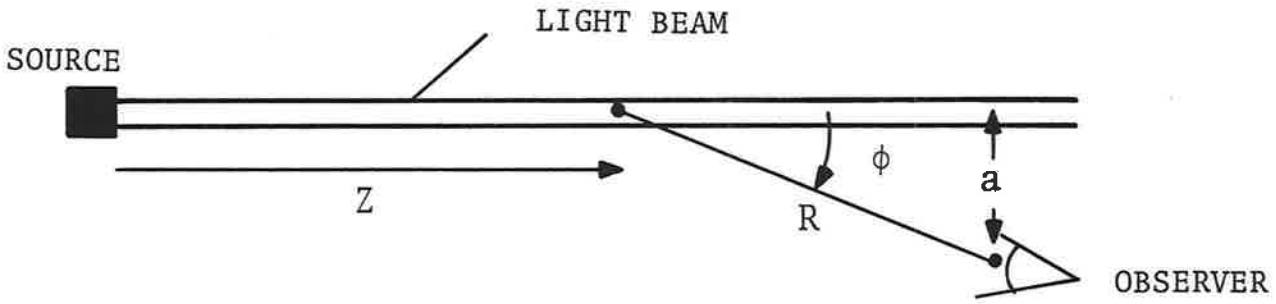

FIGURE 4. SCATTERING COORDINATES, LASER BEAM-AIDED LANDING SYSTEM CONCEPT

4. LABORATORY MEASUREMENTS AND EVALUATION

Two optically transparent receptacles were used to perform simulated atmospheric scattering measurements: a small cylindrical quartz cell (2 cm diameter x 2 cm length), and a large glass aquarium (water tank) 13"w x 16-1/2"h x 48-1/2"l. The water tank (12" x 47" inside dimension) containing a suspension of scattering particles was used to test the calculations of Section 3 and thereby lend credence to the validity of the predictions for full scale systems. Two He-Ne gas lasers of 50 and 1 mW beam power were used to generate the light beams. After the scattering behavior of several other materials was observed, it was found that diluted homogenized milk gave a reasonable simulation of scattering in the atmosphere. Table 4 shows the rough results of scattering measurements on the 2-centimeter cell containing diluted milk (transmission = 81%; σ = 10.2 m^{-1}).

TABLE 4. MEASURED VALUES OF THE RELATIVE SCATTERING FUNCTION

ϕ	$\beta'(\phi)/b$
10°	2.5
20°	1.1
35°	0.20

These results are seen to be similar to those shown in Table 3.

The water tank tests were performed with 55 ml of milk added to 140 l of water, which gave an extinction coefficient of 16.3 m^{-1}, measured across the narrow side of the tank.

An EG&G radiometer was used to make the quantitative measurements. Appropriate apertures were used to eliminate scattered light from the detector. The light transmission through the length of the tank was calculated to be 1.94 x 10^{-9}. The 1 mW laser beam source still could just be seen in the dark at this point, but it was difficult to locate one's eye in exactly the right spot because neither the 1 mW beam nor that from the 50 mW beam could be seen.

When finally located, the laser beam looked like a red star. The 1 mW He-Ne laser output corresponds to 0.15 lm. If one assumes that the eye's collecting area is a 7 mm diameter circle (3.85×10^{-5} m^2), then the effective illuminance is (0.15) x $(1.94 \times 10^{-9})/3.85 \times 10^{-5} = 7.6 \times 10^{-6}$ lm/m^2. This is just a factor of 10 above the dark threshold illuminance.

Next, the distance into the tank over which the beam could be seen by scattered light was determined in the dark. A mirror was used to reflect the beam out of the top of the tank. The mirror was moved until the beam could just be seen and the propagation distance was measured to be 99 cm. The beam diameter was 1 mm and the estimated offset of the eye to eliminate the direct beam was 5 mm. Since the angular width of the beam (1 mrad) is less than the resolution of the eye (Figure 2), we must use equation (18) to calculate the response of the eye. The result is $W_{eff}B=8.9 \times 10^{-5}$ rad . cd/m^2. We take the angular length of the beam corresponding to the far half of the beam (i.e., L = 5 mrad). The threshold on $W_{eff}B$ from Figure 3 for $B_o=10^{-2}$ is 5.3×10^{-6} rad . cd/m^2. We see that the measured threshold is a factor of 17 higher than the calculated threshold. This is reasonably good agreement considering the measurement errors involved. Moreover, the error is in the direction one would expect because of two systematic effects. First, the calculated value was for a 5/8 detection probability while the measured value was for assured detection. Second, the background adaption of the eye was probably higher than that for $B_o=10^{-2}$ because the room lights were turned off and on during the experiment. Thus we can conclude that the measurements are in reasonable agreement with the theory.

We also made some measurements of the background luminance produced by the scattered light in the tank. The flux into one end of the tank was 5.5×10^{-5} units. The scattered light was measured at the other end of the tank 1 m away from an estimated area of 1.14×10^{-3} m^2 and solid angle of 0.35 sr. The result was 5.9×10^{-10} units. The measured ratio of luminance B to flux F is

0.027. From equation (4), one calculates a ratio of 0.025 which agrees almost too well. One should note that the measured luminance from the side of the tank near the end was a factor of four less than that on the end. This result is in rough agreement with the use of Lambert's law for the distribution of radiation.

5. PATH CLEARANCE THROUGH FOG

Consider the power required from a CO_2 laser to clear a path through a fog so that a visible light beam can be propagated up to a pilot. The first question to be answered is how much energy is required to evaporate the fog in a volume of air. The minimum energy is the heat of vaporization of the water droplets which is about 2500 J/g. In addition, it may be necessary to raise the air temperature to the equilibrium level for no condensation. The temperature rise for a given liquid water density can be determined from Figure 5, which plots the water vapor density versus the dew point. The specific heat of air is about 950 J/m^3. The liquid water density of a dense fog is typically 0.1 g/m^3 and could be as large as 0.2 or 0.3 g/m^3. Based on the value 0.1 g/m^3, the relevent parameters are shown in Table 5.

TABLE 5. ENERGY DENSITY TO CLEAR FOG (0.1 g/m^3)

TEMPERATURE	HEAT OF VAPORIZATION	EQUILIBRIUM TEMPERATURE RISE	HEAT TO RAISE TEMPERATURE
0°C	250 J/m^3	0.45°C	430 J/m^3
20°C	250 J/m^3	0.11°C	100 J/m^3

For estimating purposes assume an energy density of 500 J/m^3.

We now need to model the effects of beam propagation. We are helped significantly by the much stronger absorption of liquid water compared with water vapor. The beam will tend to clear a region out to a point where most of the energy is absorbed. Consider a region 2 km long and 0.3 x 0.3 m^2 in cross section. The volume of such region is 180 m^3 and would require 90,000 J to clear. The time required for the delivery of this much energy is roughly the dimension of the beam divided by the crosswind. For a 3 m/s (~6 kts) crosswind, the time is 0.1 sec. The required laser power is thus about 1 MW cw. The availability of lasers of this magnitude for non-military activities is uncertain. In any case, they

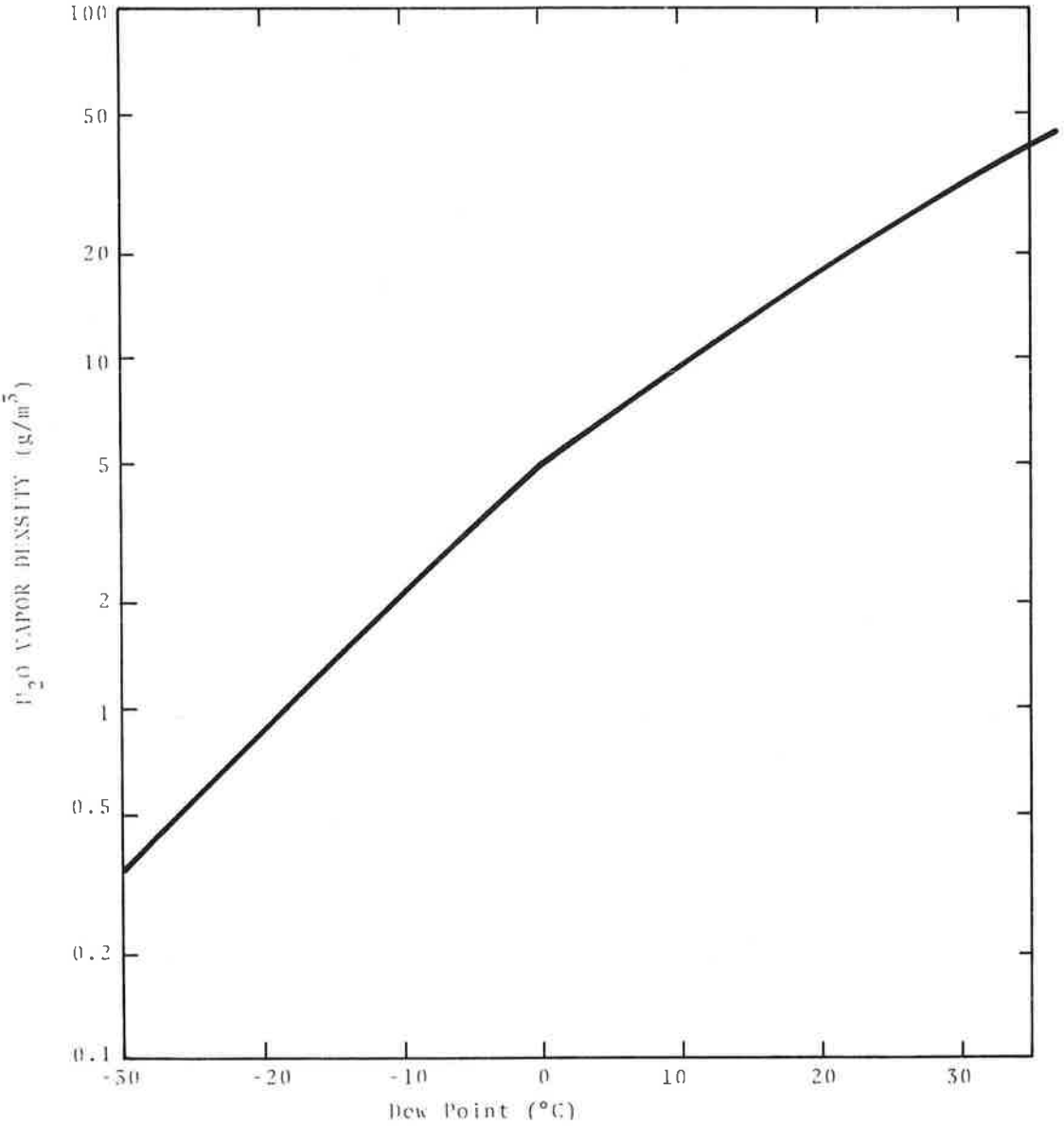

FIGURE 5. VAPOR DENSITY VERSUS DEW POINT OF WATER

would pose a severe hazard to the pilot if not the aircraft. This calculation has assumed optimistically that all the CO_2 laser power is absorbed and that heating effects will not destroy the beam collimation. A significant fraction of the light will be scattered (1/2 by the optical theorem of scattering for large particles), and the heating will likely defocus the beam. See [8] for a more complete discussion of this problem.

6. LASER BEAM SAFETY

One of the major goals of this program has been to determine if lasers can be safely used to provide visual guidance to pilots for all aircraft operations. The concern for pilot safety is that many of the landing system concepts considered require the pilot to look at visible laserbeams. A visible laserbeam can, in theory, be focused on the human retina to an image size that approaches the dimensions of the laser wavelength so that even at low power exposures an eye hazard exists. For this reason a scenario has been developed to establish the magnitude of pilot exposure to laser radiation for each system concept considered. The criteria for evaluating eye-safe operation were taken directly from the laser products performance standard of the Department of Health, Education, and Welfare -- Food and Drug Administration (Federal Standard [9]).

6.1 FEDERAL STANDARD

Under authority of the Public Health Service Act as amended by the radiation control for the Health and Safety Act of 1968, Chapter I of Title 21 of the Code of Federal Regulations was amended by adding a new part, 1040, to Subchapter J, prescribing a radiation safety performance standard for laser products. The purpose of this standard is "to protect the public health and safety from the danger of laser radiation . . . by reducing the possibility of injury by minimizing unnecessary accessible radiation."

The standard became effective 2 August 1976, and it established the classification of all laser products according to the emission level, duration, and wavelength(s) of accessible laser radiation emitted during the operation of the laser. Accessible emission limits were specified for each of four classes: from Class I laser products, which cannot, under normal operating conditions, emit a hazardous level of radiation; to Class IV lasers, which can be extremely hazardous to eye or skin, not only

from direct beam exposure but also from the scattered beam. Tables 6 through 10 were taken from the Federal Standard and show the accessible emission limits for each class with the correction factors k_1 and k_2.

6.2 HAZARD ANALYSIS

The hazard posed to a pilot by a visible laser guidance system will be analyzed by considering the system concept depicted in Figure 6: An aircraft is making an instrument landing (ILS) approach to an airport runway. At some point before reaching the decision height the pilot views a pair of parallel lightbeams emanating from the ground. Visibility permitting, he positions his aircraft between the two beams, descends visually, and lands. Using this scenario, the potential hazard conditions are the chance direct viewing of one of the laserbeam sources from within the beam (intrabeam viewing) and the steady side viewing (extrabeam viewing) of the two beams during the descent. The potential radiation hazard at the source (i.e., the ground-based transmitter) is effectively removed, by either elevating the laser source to a height above eye level, or increasing the diameter of the transmitted beam.

In the following calculations the level of radiation that can be safely viewed is made equal to the accessible emission limit of a Class I laser product* whose emission wavelength is >400 but $\leq$1400 nm, and whose emission durations are from 2.0×10^{-5} to 1.0×10^{1} sec and from 1.0×10^{1} to 1.0×10^{4} sec. From Table 6, these limits are $7.0 \times 10^{-4}\ k_1 k_2 t^{3/4}$ and $3.9 \times 10^{-3}\ k_1 k_2$ and from Table 9, k_1 and k_2 are both equal to 1.0. Thus, the maximum levels of laser energy allowed are $I_{mx}(t) = 7.0 \times 10^{-4}$ J, in $t^{3/4}$ sec (for $t > 2.0 \times 10^{-5}$ to 1.0×10^{1} sec), and $I_{mx} = 3.9 \times 10^{-3}$ J. The observer is assumed to have

*By restricting the level of radiation to the accessible emission limit of a Class I laser, a minimum risk of eye injury to a pilot is assured.

TABLE 6. CLASS I ACCESSIBLE EMISSION LIMITS FOR LASER RADIATION

Wavelength (nanometers)	Emission duration (seconds)	Class I – Accessible emission limits
> 250 but ≤400	$\leq 3.0 \times 10^{4}$	$2.4 \times 10^{-5} k_1 k_2$ J*
	$> 3.0 \times 10^{4}$	$8.0 \times 10^{-10} k_1 k_2 t$ J
> 400 but ≤ 1400	$> 1.0 \times 10^{-9}$ to 2.0×10^{-5}	$2.0 \times 10^{-7} k_1 k_2$ J
	$> 2.0 \times 10^{-5}$ to 1.0×10^{1}	$7.0 \times 10^{-4} k_1 k_2 t^{3/4}$ J
	$> 1.0 \times 10^{1}$ to 1.0×10^{4}	$3.9 \times 10^{-3} k_1 k_2$ J
	$> 1.0 \times 10^{4}$	$3.9 \times 10^{-7} k_1 k_2 t$ J
	OR**	
	$> 1.0 \times 10^{-9}$ to 1.0×10^{1}	$10 k_1 k_2 t^{1/3}$ J cm^{-2} sr^{-1}
	$> 1.0 \times 10^{1}$ to 1.0×10^{4}	$20 k_1 k_2$ J cm^{-2} sr^{-1}
	$> 1.0 \times 10^{4}$	$2.0 \times 10^{-3} k_1 k_2 t$ J cm^{-2} sr^{-1}
> 1400 but ≤ 13000	$> 1.0 \times 10^{-9}$ to 1.0×10^{-7}	$7.9 \times 10^{-5} k_1 k_2$ J
	$> 1.0 \times 10^{-7}$ to 1.0×10^{1}	$4.4 \times 10^{-3} k_1 k_2 t^{1/4}$ J
	$> 1.0 \times 10^{1}$	$7.9 \times 10^{-4} k_1 k_2 t$ J

* Class I accessible emission limits for the wavelength range of greater than 250 nm but less than or equal to 400 nm shall not exceed the Class I accessible emission limits for the wavelength range of greater than 1400 nm but less than or equal to 13000 nm with a k_1 and k_2 of 1.0 for comparable sampling intervals.

** Instructions for the Class I dual limits are set forth in paragraph (d)(4) of this section.

TABLE 7. CLASS II ACCESSIBLE EMISSION LIMITS FOR LASER RADIATION

Wavelength (nanometers)	Emission duration (seconds)	Class II – Accessible emission limits
> 400 but ≤ 710	$> 2.5 \times 10^{-1}$	$1.0 \times 10^{-3} k_1 k_2 t$ J

TABLE 8. CLASS III ACCESSIBLE EMISSION LIMITS FOR LASER RADIATION

Wavelength (nanometers)	Emission duration (seconds)	Class III – Accessible emission limits
> 250 but ≤ 400	$\leq 2.5 \times 10^{-1}$	$3.8 \times 10^{-4} k_1 k_2$ J
	$> 2.5 \times 10^{-1}$	$1.5 \times 10^{-3} k_1 k_2 t$ J
> 400 but ≤ 1400	$> 1.0 \times 10^{-9}$ to 2.5×10^{-1}	$10 k_1 k_2 t^{1/3}$ J cm^{-2} to a maximum value of 10 J cm^{-2}
	$> 2.5 \times 10^{-1}$	$5.0 \times 10^{-1} t$ J
≥ 1400 but ≤ 13000	$> 1.0 \times 10^{-9}$ to 1.0×10^{1}	10 J cm^{-2}
	$> 1.0 \times 10^{1}$	$5.0 \times 10^{-1} t$ J

TABLE 9. VALUES OF WAVELENGTH DEPENDENT CORRECTION FACTORS k_1 AND k_2

Wavelength (nanometers)	k_1	k_2		
250 to 302.4	1.0	1.0		
> 302.4 to 315	$10^{\left[\frac{\lambda - 302.4}{5}\right]}$	1.0		
> 315 to 400	330.0	1.0		
> 400 to 700	1.0	1.0		
> 700 to 800	$10^{\left[\frac{\lambda - 700}{515}\right]}$	if: $t \leq \frac{10100}{\lambda - 699}$ then: $k_2 = 1.0$	if: $\frac{10100}{\lambda - 699} < t \leq 10^4$ then: $k_2 = \frac{t(\lambda - 699)}{10100}$	if: $t > 10^4$ then: $k_2 = \frac{\lambda - 699}{1.01}$
> 800 to 1060	$10^{\left[\frac{\lambda - 700}{515}\right]}$	if: $t \leq 100$ then: $k_2 = 1.0$	if: $100 < t \leq 10^4$ then: $k_2 = \frac{t}{100}$	if: $t > 10^4$ then: $k_2 = 100$
> 1060 to 1400	5.0			
> 1400 to 1535	1.0	1.0		
> 1535 to 1545	$t \leq 10^{-7}$ $k_1 = 100.0$	1.0		
	$t > 10^{-7}$ $k_1 = 1.0$			
> 1545 to 13000	1.0	1.0		

Note: The variables in the expressions are the magnitudes of the sampling interval (t), in units of seconds, and the wavelength (λ), in units of nanometers.

TABLE 10. SELECTED NUMERICAL SOLUTIONS FOR k_1 AND k_2

Wavelength (nanometers)	k_1	k_2				
		$t \leq 100$	$t = 300$	$t = 1000$	$t = 3000$	$t \geq 10{,}000$
250	1.0					
300	1.0					
302	1.0					
303	1.32					
304	2.09					
305	3.31					
306	5.26					
307	8.32					
308	13.2					
309	20.9					
310	33.1			1.0		
311	52.5					
312	83.2					
313	132.0					
314	209.0					
315	330.0					
400	330.0					
401	1.0					
600	1.0					
800	1.0					
700	1.0					
710	1.05	1	1	1.1	3.3	11.0
720	1.09	1	1	2.1	6.3	21.0
730	1.14	1	1	3.1	9.3	31.0
740	1.20	1	1.2	4.1	12.0	41.0
750	1.25	1	1.5	5.0	15.0	50.0
760	1.31	1	1.8	6.0	18.0	60.0
770	1.37	1	2.1	7.0	21.0	70.0
780	1.43	1	2.4	8.0	24.0	80.0
790	1.50	1	2.7	9.0	27.0	90.0
800	1.56	1	3.0	10.0	30.0	100.0
850	1.95	1	3.0	10.0	30.0	100.0
900	2.44	1	3.0	10.0	30.0	100.0
950	3.05	1	3.0	10.0	30.0	100.0
1000	3.82	1	3.0	10.0	30.0	100.0
1050	4.78	1	3.0	10.0	30.0	100.0
1060	5.00	1	3.0	10.0	30.0	100.0
1100	5.00	1	3.0	10.0	30.0	100.0
1400	5.00	1	3.0	10.0	30.0	100.0
1500	1.0					
1540	100.0*			1.0		
1600	1.0					
13000	1.0					

*The factor $k_1 = 100.0$ when $t \leq 10^{-7}$, and $k_1 = 1.0$ when $t > 10^{-7}$

Note: The variable (t) is the magnitude of the sampling interval in units of seconds.

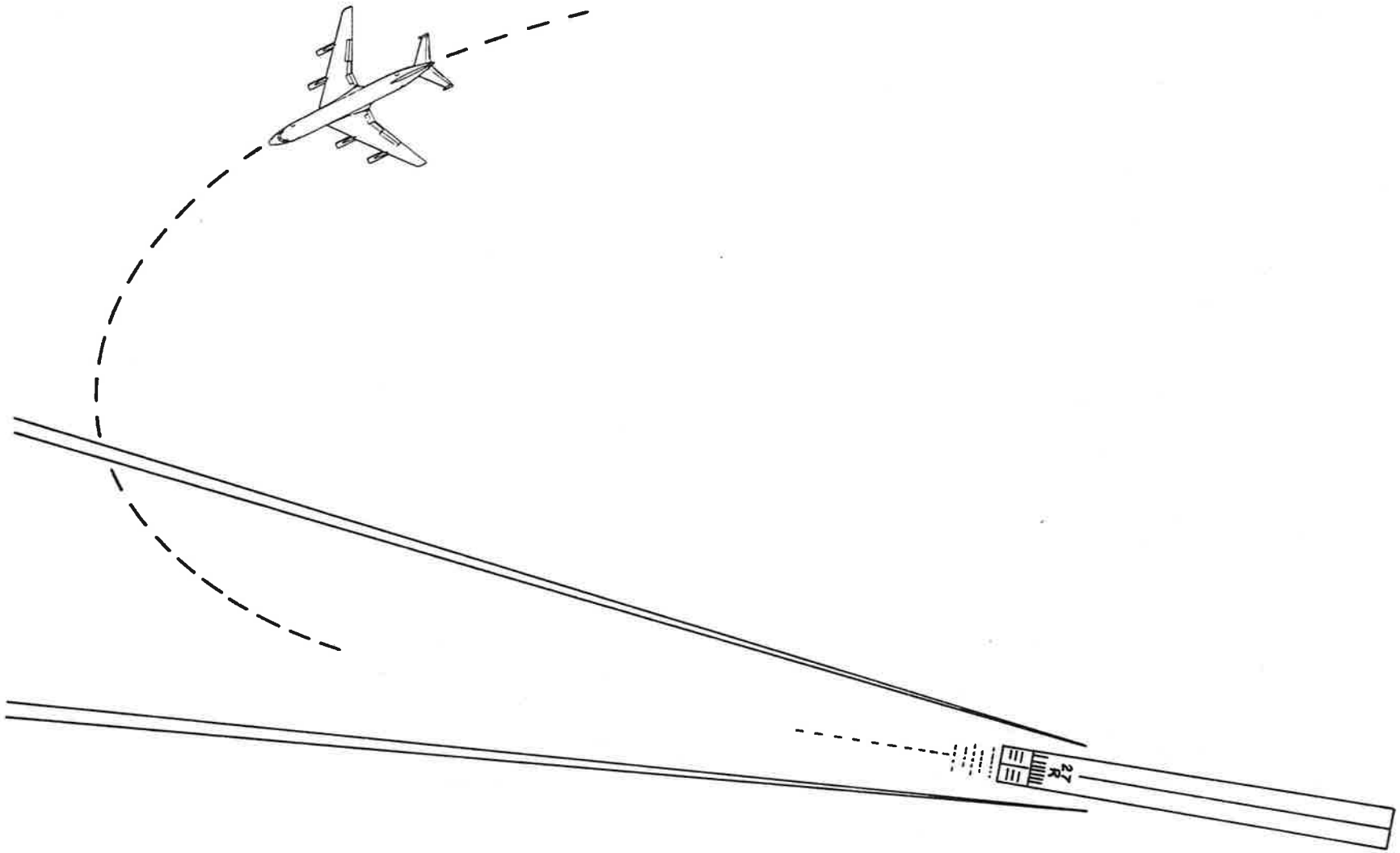

FIGURE 6. LASER-AIDED LANDING SYSTEM CONCEPT

dark-adapted vision so that the pupil of the eye is fully dilated (7 mm pupil diameter).

The total time that the pilot's eyes are irradiated for each type of viewing (i.e., intrabeam or extrabeam) must be determined. Intrabeam viewing, in the above scenario, is not intended to be for extended periods, but rather the result of chance viewing as during aircraft positioning for an approach. For beam diameters of 30 to 90 cm, and aircraft speeds of 60 to 160 kts, exposures of 0.004 to 0.03 sec are expected.

For the extrabeam viewing case the pilot is continuously exposed to that portion of laserbeam radiation scattered towards him during his landing approach. If it is assumed that the pilot has visually acquired the parallel laserbeams at the middle marker and is approaching the touchdown point at a speed of 80 kts (177 ft/sec), his exposure time is approximately 25 sec (distance from middle marker to touchdown, ~ 4500 ft).

Now that the exposure time has been determined for each viewing condition the irradiance limit (H_L) may be calculated. However, for added safety the exposure time (τ) is arbitrarily increased to intrabeam = 1.0 sec, extrabeam = 250 sec. Then the retinal irradiance limit is given by

$$H_L = \frac{I_{mx}(t)}{\tau \cdot A_E} \quad , \tag{20}$$

where A_E is the area of a dark adapted eye (7.0 mm pupil diameter).

$$H_L = \frac{7.0 \times 10^{-4} \text{ W-sec}}{1.0 \text{ sec } (0.385) \text{ cm}^2}$$

(intrabeam) $$H_L = 0.002 \frac{\text{W}}{\text{cm}^2} \text{ or } 20 \frac{\text{W}}{\text{M}^2} \tag{21}$$

and $$H_L = \frac{I_{mx}}{\tau \cdot A_E}$$

$$H_L = \frac{3.9 \times 10^{-3} \text{ W sec}}{250 \text{ sec } (0.385) \text{ cm}^2}$$

(extrabeam) $$H_L = 4 \times 10^{-5} \text{ W/cm}^2 \text{ or } 0.4 \text{ W/M}^2 \quad . \tag{22}$$

6.3 OPERATIONAL SAFETY CONSIDERATIONS

The amount of radiation incident on the eye of an intrabeam observer/pilot will vary according to the relation

$$H_R = \frac{4\ P_t e^{-\sigma R}}{\pi\left(\frac{4R\lambda}{\pi D_t} + D_t\right)^2} \quad . \tag{23}$$

Where P_T is the laser power out of the transmitter optics of diameter D_T, σ is the mean extinction coefficient, R is the distance from the laser source to observer, and λ is the emission wavelength. Figure 7 shows H_R for the parameters P_T, D_T, and R. The broken line separates the safe region (below) from the hazardous one (above).

For the extrabeam observer, the amount of radiation viewed has been shown to be below the day detection threshold of the observer (see Section 7.2, Figure 11). The day detection threshold is 5.72×10^{-7} W/M^2, which is well below the retinal irradiance limit (see Section 2.2). Therefore, the extrabeam eye hazard can be safely ignored.

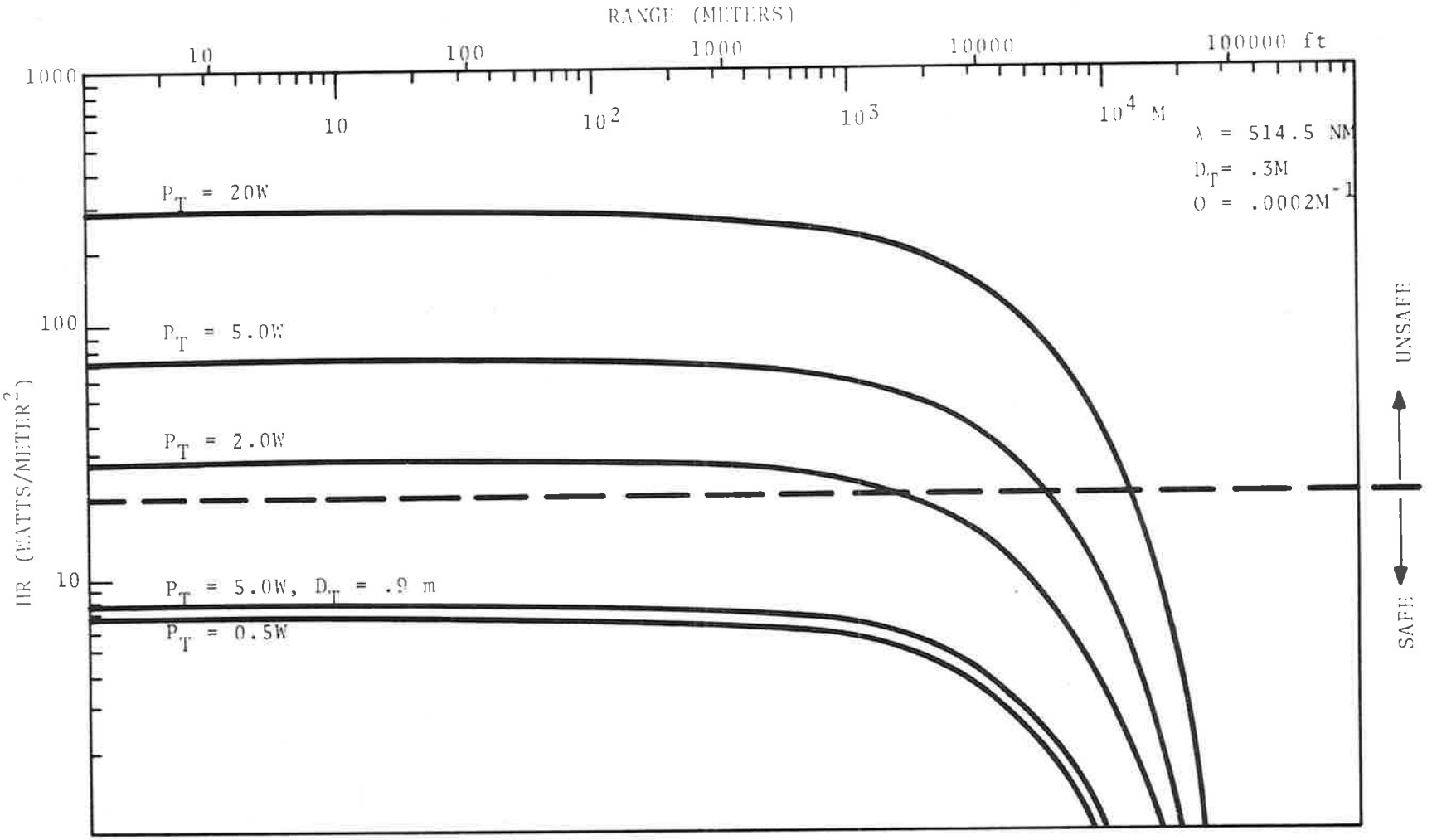

FIGURE 7. INTRABEAM VIEWING

7. FEASIBILITY OF SYSTEM CONFIGURATIONS

The feasibility of using a laser lighting system to assist aircraft landing under low-visibility conditions was evaluated analytically using the newly developed model for viewing line sources (light beams). The following sections describe the results.

7.1 SYSTEM CONCEPTS

The US patent (#4,063,218) on the Russian Glissada system considers a multitude of embodiments, all of which are designed to have the pilot view the light beam(s) by light scattered at a small angle. Such systems have the virtue that small scattering angles give the strongest signals, and a small number of beams can cover a large region of space. They suffer, however, from two major disadvantages. First, the beam source must be far away from the pilot so that attenuation is a problem under conditions of poor visibility. Second, the aircraft can fly into the beam so that the pilot's eyes become exposed to the direct beam intensity.

During the course of the work reported here, we studied a second type of system based on viewing light beams by light scattered at large scattering angles. The two major virtues of such systems are that the distance from the source to the pilot can be much shorter than in the Glissada systems and that the pilot cannot view the beam directly because it is below the cockpit cutoff angle. Figures 8 and 9 show two ways of implementing this concept. The first consists of a line of vertically pointing beams marking the runway centerline. Such an arrangement may be more useful for ground guidance than for approach guidance since it gives no indication of aircraft deviations from the glideslope. The second approach (Figure 9) marks both the glidescope and runway centerline by intersecting beams of light. Both of these approaches suffer from the requirement of a large number of lights. However, the short distance from the light source to the

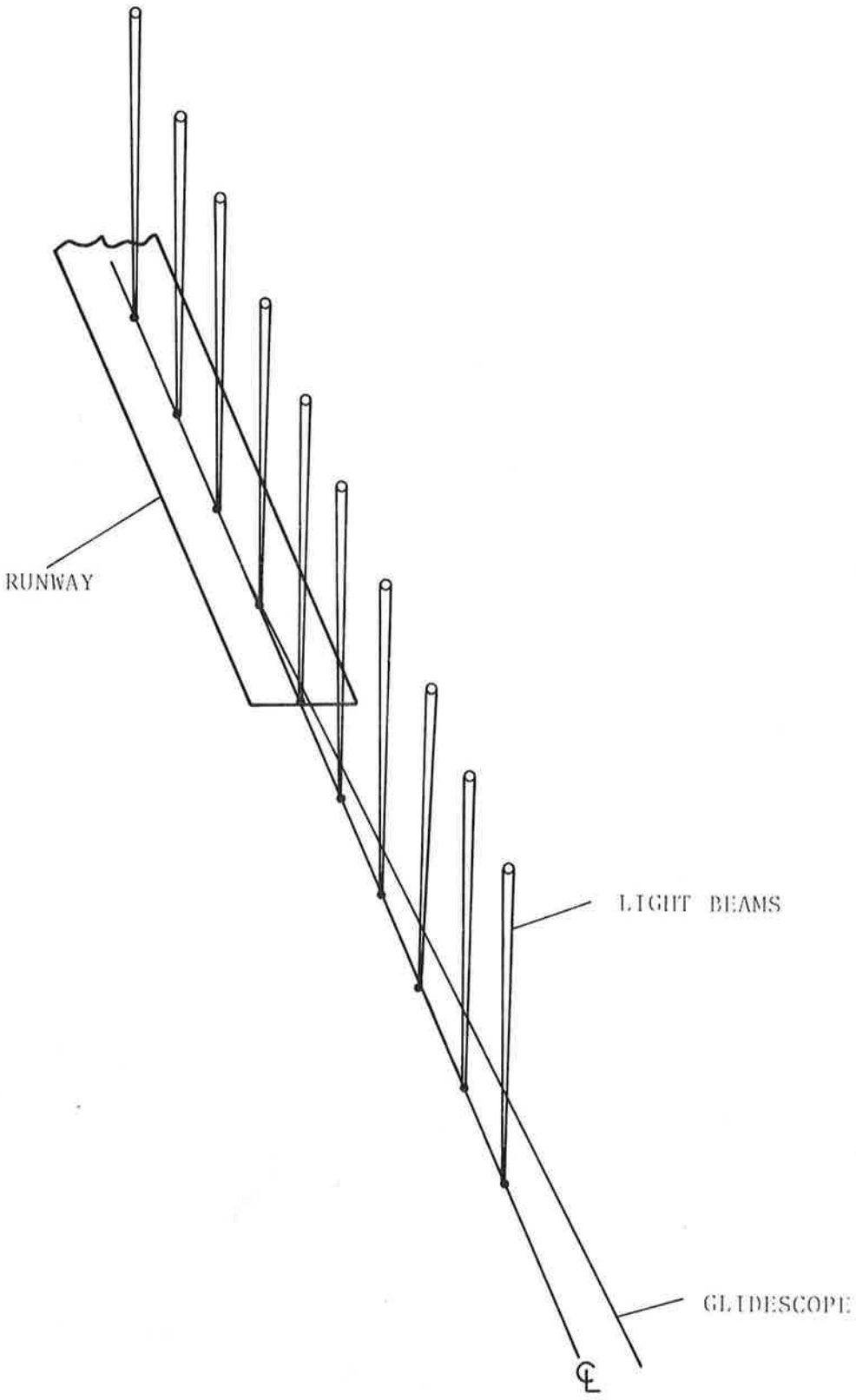

FIGURE 8. NARROW LIGHT BEAMS ARRANGED IN A CLOSE-SPACED ARRAY DOWN THE CENTERLINE OF THE RUNWAY

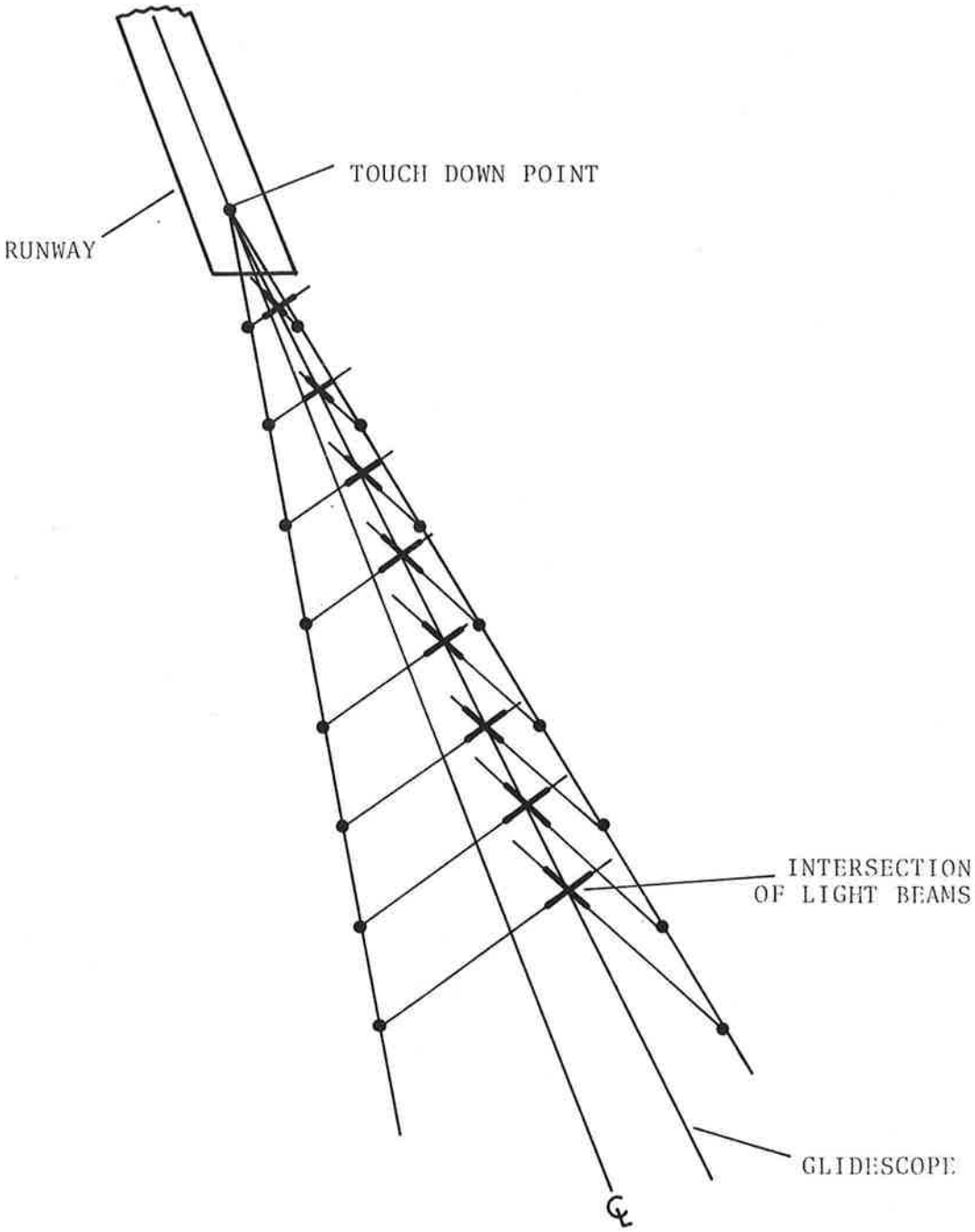

FIGURE 9. NARROW LIGHT BEAM PAIRS INTERSECTING AT THE GLIDEPATH

point viewed allows the use of inexpensive spot lights rather than lasers to generate the beams. (See Appendix B for a comparison of lasers and conventional light sources.) Because the light scattering in the atmosphere is skewed toward the forward direction, it is advantageous to tilt the beams toward the pilot rather than using 90° viewing as shown in Figures 8 and 9.

In the next section the system capabilities are calculated for one Glissada system and one large angle system.

7.2 SYSTEM ANALYSIS

One of the many possible approach lighting system concepts is shown in Figure 10. Narrow light beams on either side of the runway mark the glide slope and runway location. To determine the detectability of such beams under different visibility conditions, we assume that the beams are displaced by 76 m (250 ft) from the runway centerline and that two argon gas lasers* of 2 watts (1000 lm) output power are located 366 m (1200 ft) beyond the runway threshold. Also, we assume that the beams must be visible from the middle marker location 1067 m (3500 ft) before the runway threshold. We take the beam diameter as 0.30 m (1 ft). At this distance (1433 m) the beam is much narrower than the resolution (visual angle) of the eye (Figure 2), so we must use equation (18). The angular length of the beam is roughly 76/1433 = 53 mrad. The resulting detection thresholds for backgrounds (B_o) day ($B_o=10^4$) and night ($B_o=10^{-2}$) are (from Figure 3) 7.6×10^{-2} and 2.4×10^{-6}, respectively. The results are plotted in Figures 11 and 12. The RVR threshold for seeing the beam is slightly below 4000 ft at night. The beam cannot be seen during bright daylight.

For comparison, consider a second system concept shown in Figure 13. In this system a pilot views two crossing narrow beams coming up at an angle of 45° from his line of sight. At the middle marker the aircraft altitude is about 60 m. The distance

---

*Argon gas lasers are used in these calculations because they are commercially available in the higher CW-power ranges.

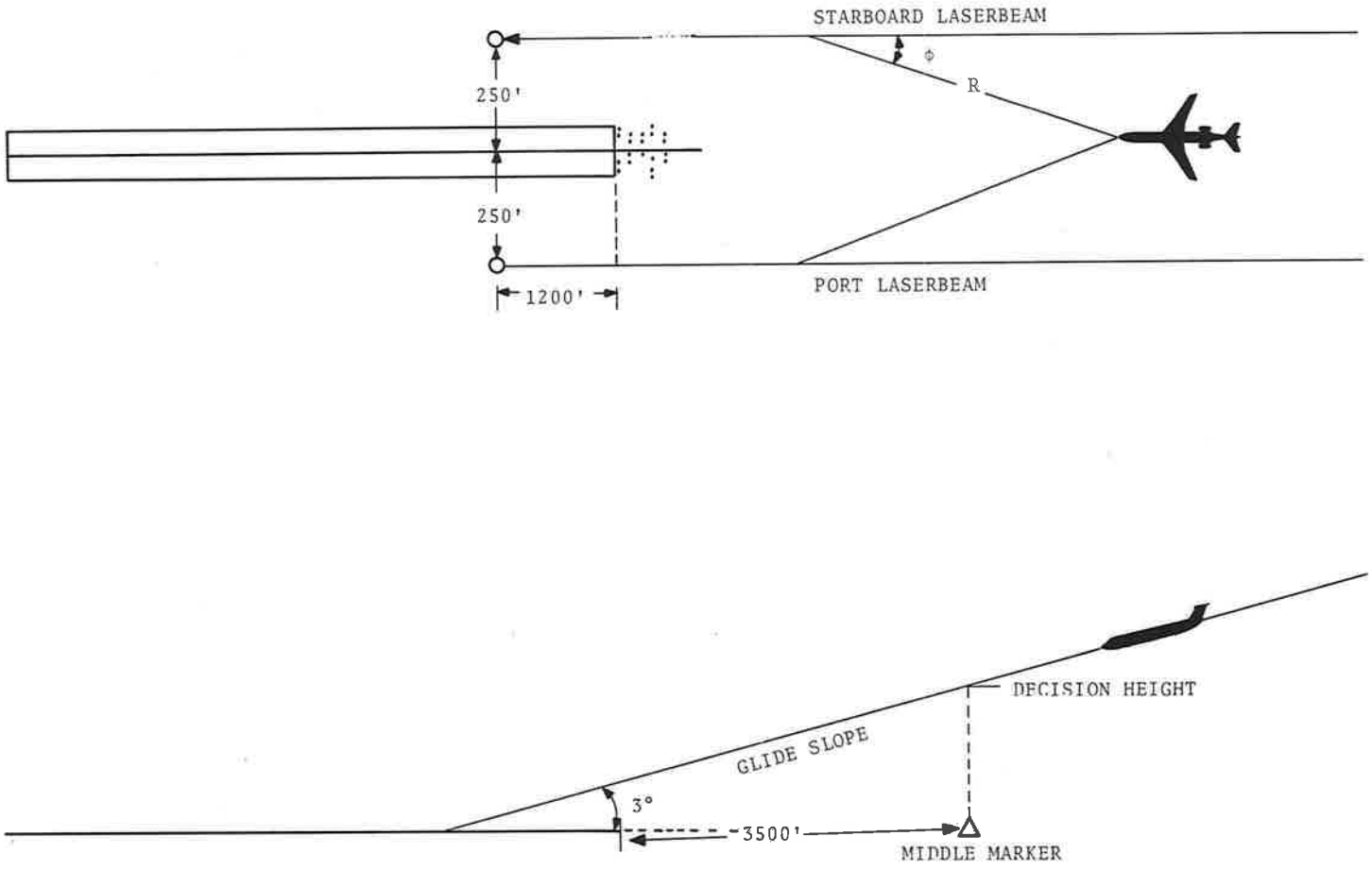

FIGURE 10. LASERBEAM APPROACH LIGHTING SYSTEM

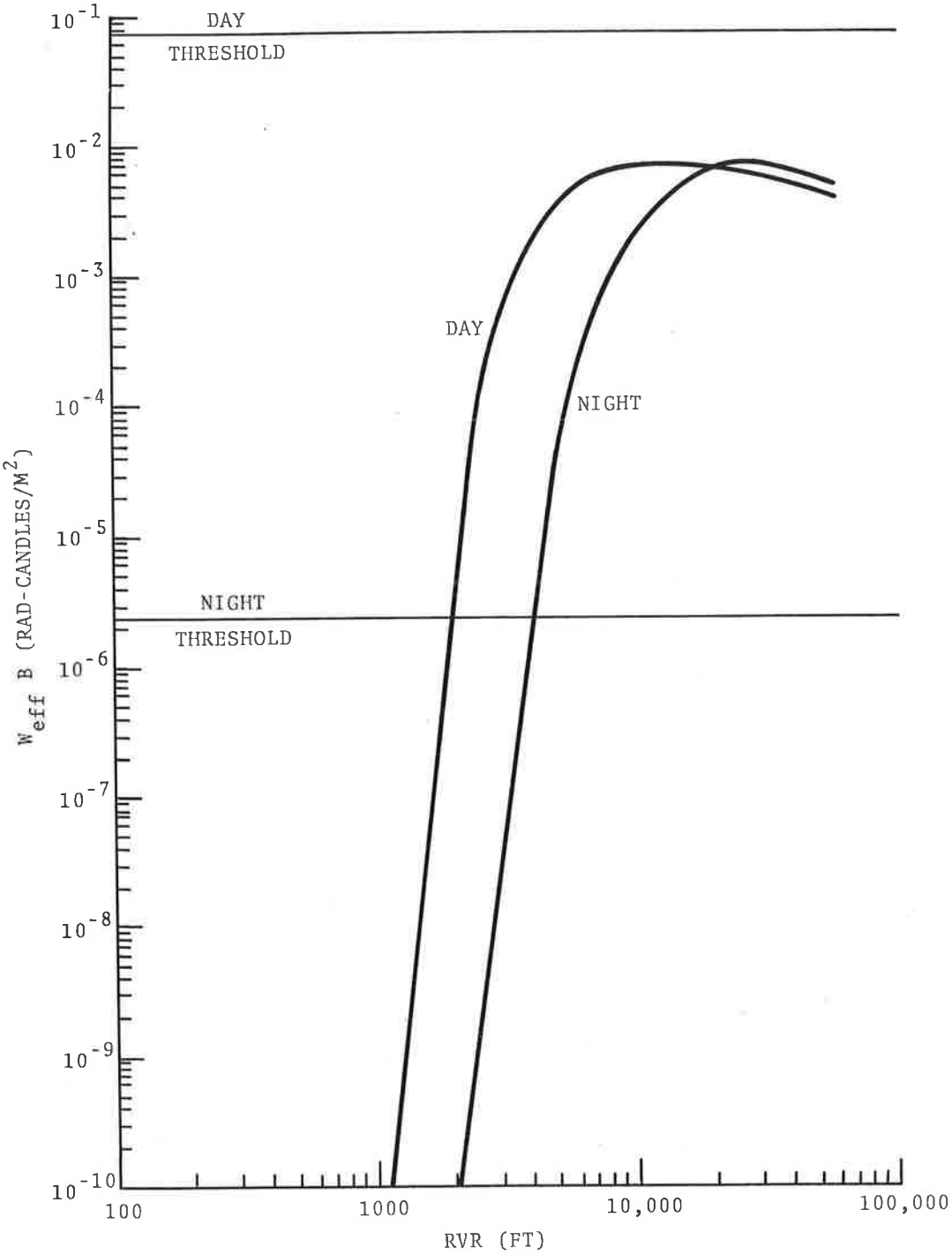

FIGURE 11. GLISSADA SYSTEM PERFORMANCE

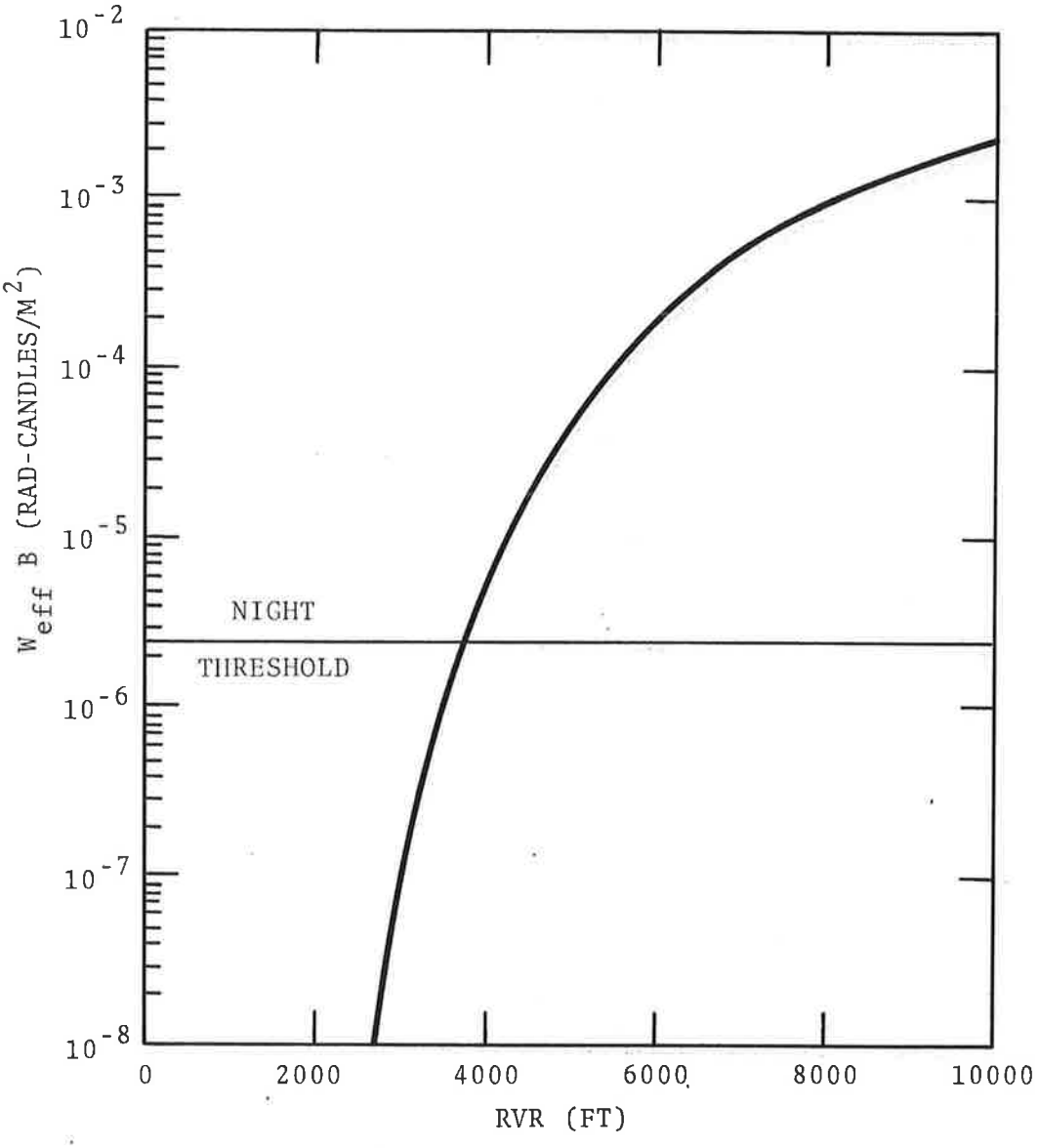

FIGURE 12. GLISSADA SYSTEM PERFORMANCE, EXPANDED SCALE

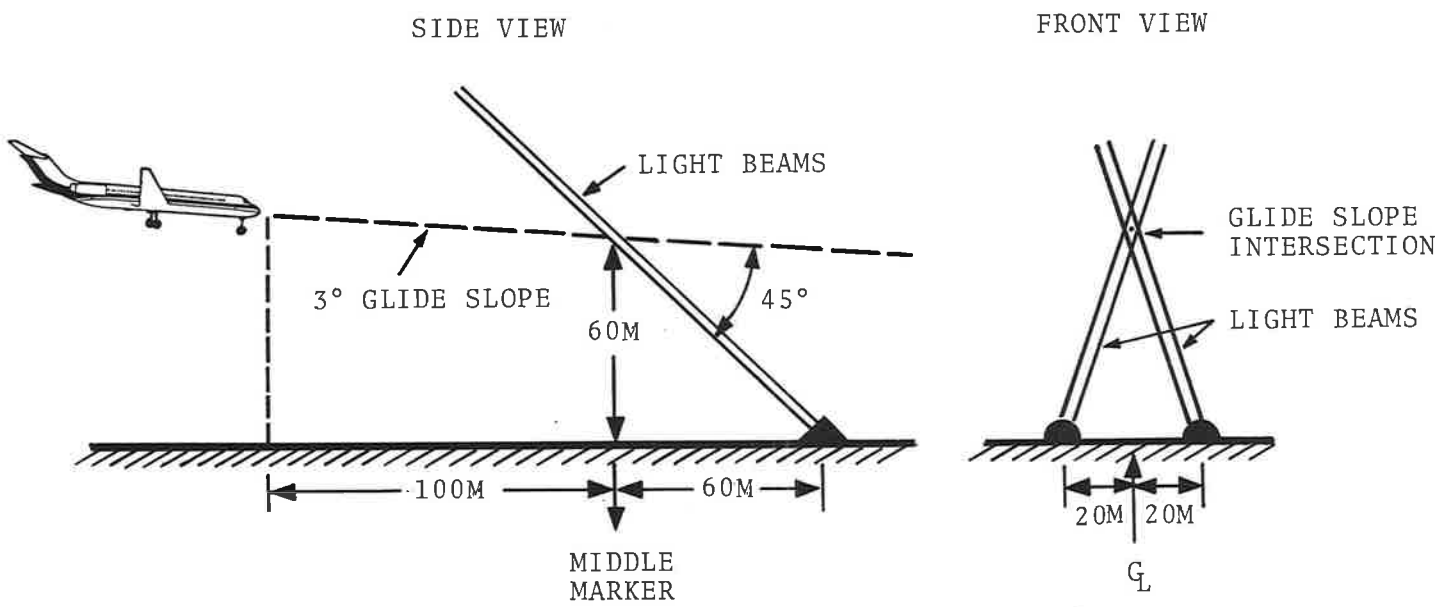

FIGURE 13. SECOND SYSTEM CONCEPT

from the light source to the point viewed (z) is 85 m. Assume that the pilot must see the intersection of the beam pair from 100 m away and the beam diameters from 0.3 m away. The angular width is 3 mrad, which is below the night eye resolution but above that for the day ($\Delta\phi$ = 0.8 mrad). Thus we use equation (18) for night and equation (19) for day. Figures 14, 15, and 16 are plots of the results for a 2W Ar^+ ion laser beam for two viewing distances, 100 m and 200 m. The relevant angular length of the beam in this case is perhaps 0.2 rad. The corresponding threshold is about 0.05×10^{-6} and 1.6×10^{-6} for day and night, respectively. These beams are thus never visible in the daylight but are quite visible at night even below the Category IIIa minimum of 700 ft RVR. The results show that the signal actually reaches a maximum for a particular RVR and decreases for both smaller and larger values. This effect is caused by the two-fold effect of the scattering. The scattering process produces the signal but it also attenuates the beam.

A comparison of these two examples shows that it pays to bring the light source closer to the observer even if it means that other parameters such as the scattering function β' are decreased.

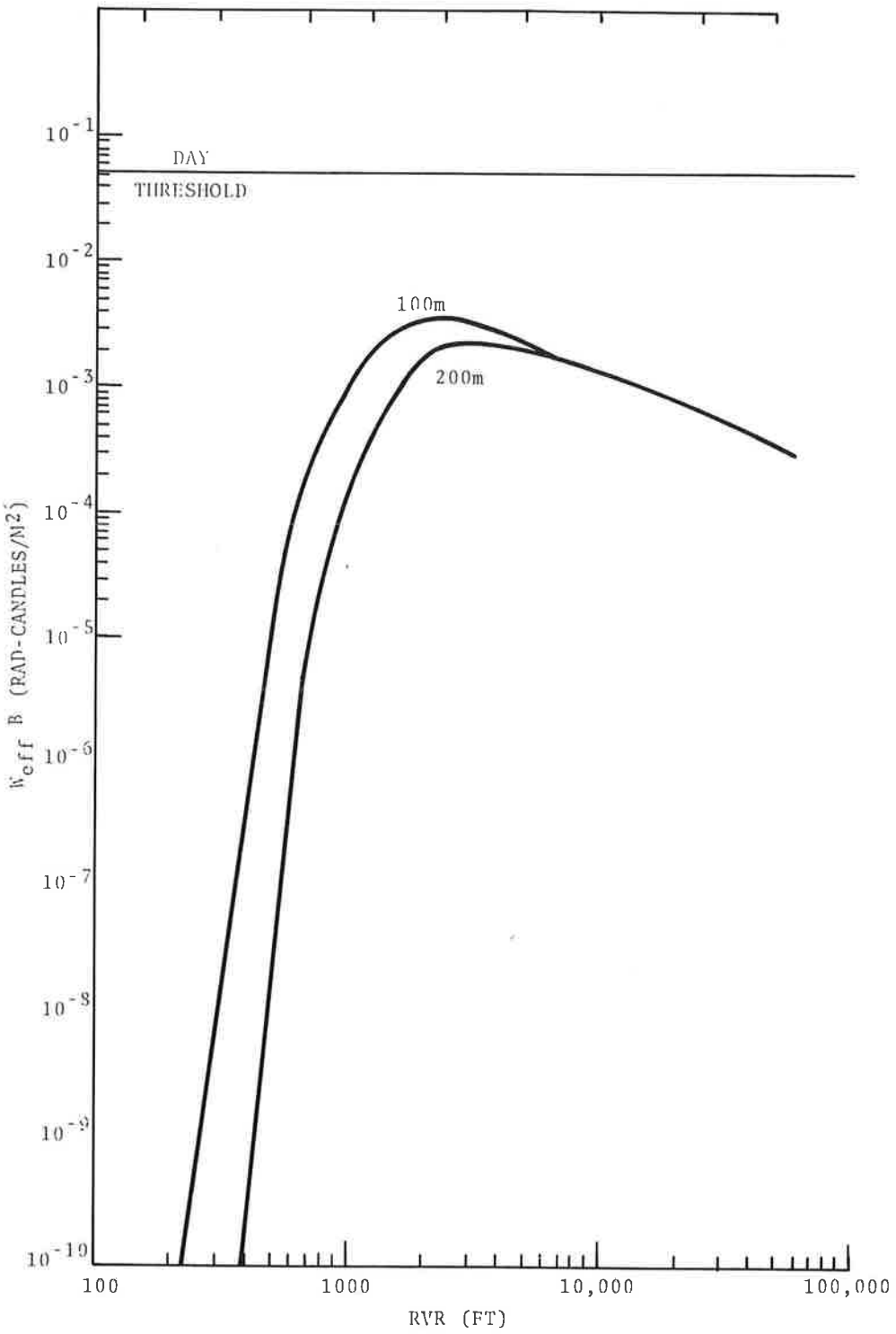

FIGURE 14. SECOND SYSTEM PERFORMANCE, DAYTIME

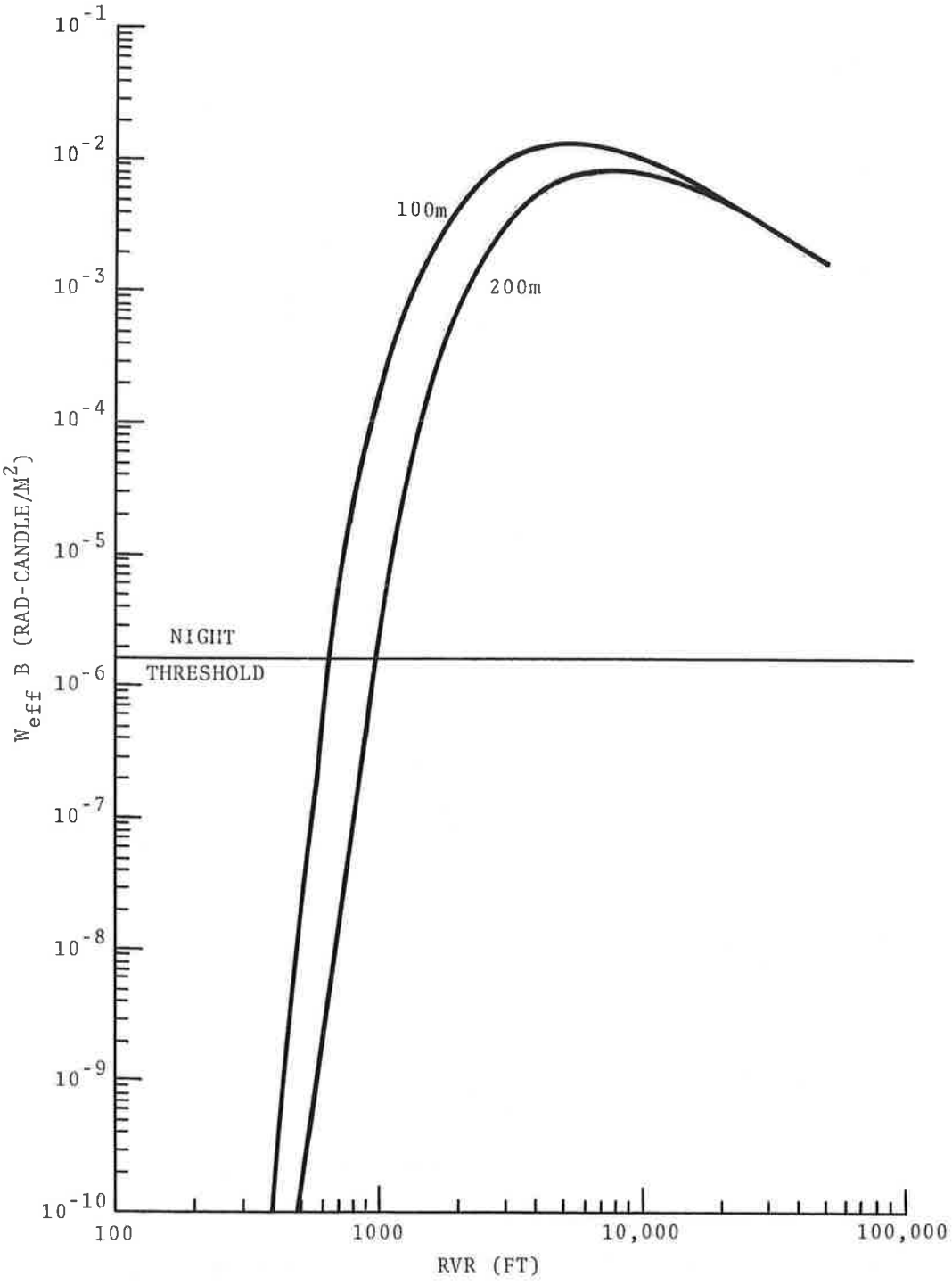

FIGURE 15. SECOND SYSTEM PERFORMANCE, NIGHTTIME

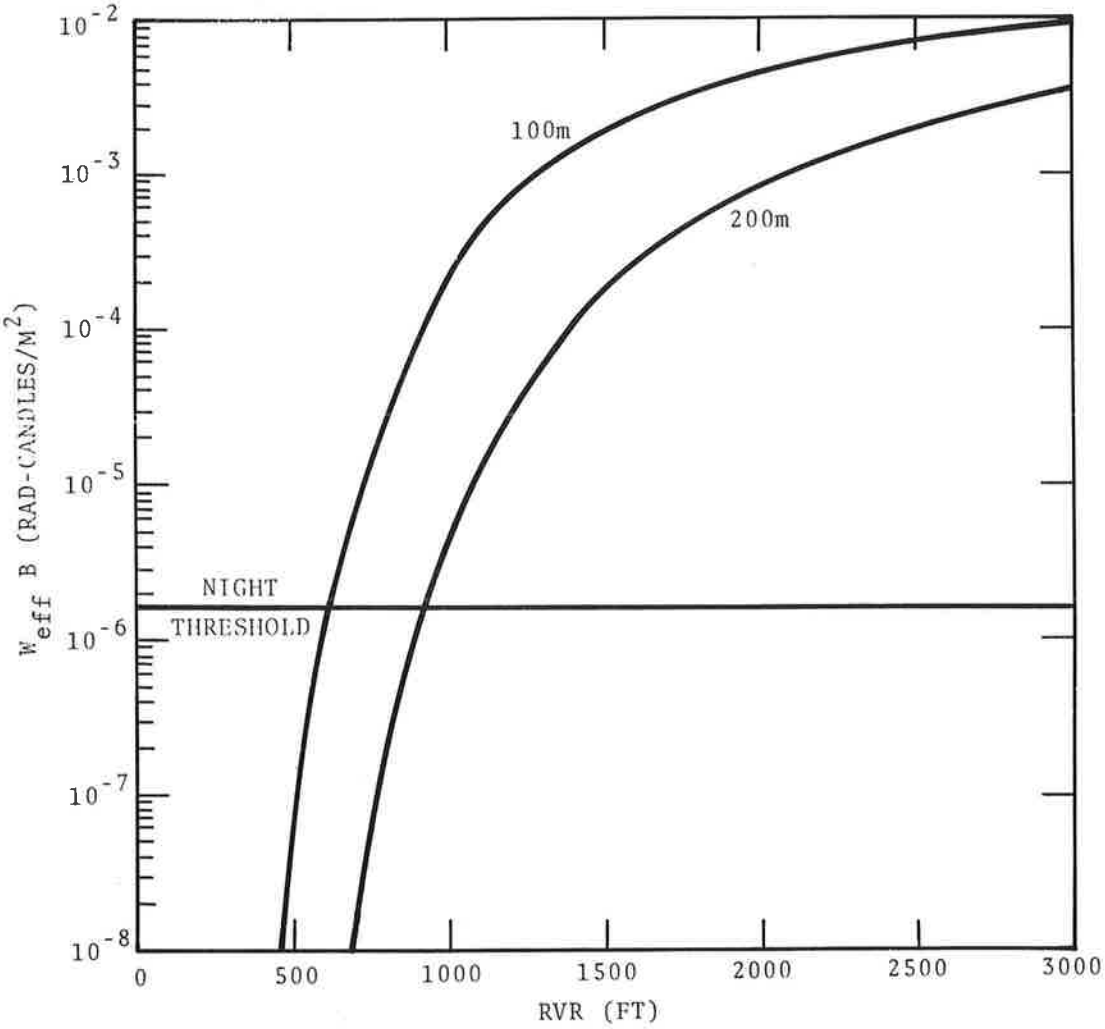

FIGURE 16. COMPARISON SYSTEM PERFORMANCE, EXPANDED SCALE (NIGHTTIME)

8. CONCLUSIONS

A model for the visual detectability of narrow light beams was developed and used to evaluate the system performance of two laser lighting system configurations: The first configuration, consisting of two narrow beam laser sources placed at the VASI (Visual Approach Slope Indicator) locations, was found to be useful only for RVR(s) (Runway Visual Ranges) greater than 4000 ft (assuming uniform visibility up the glidescope). The second configuration, consisting of a pair of laser beams pointing to and intersecting with the flight path at a 45° angle, was found to be visible from a distance of 300 ft away for RVR(s) greater than 700 ft.

Laboratory experiments confirmed the validity of the model. Results of laboratory scattering measurements compared well with data presented by Middleton [6].

The analysis indicated that using an infrared laser to clear a path through fog poses serious problems; continuous powers greater than 1 MW are required.

Using a criterion taken from the Federal Standard for laser safety, the potential hazards of each of the system concepts were evaluated. For the extrabeam observer (i.e., one who views the scattered light) the potential hazard is insignificant. However, the eye safety of the intrabeam observer must be taken into consideration as a system design requirement.

9. RECOMMENDATIONS

Although the Glissada type system with two glideslope beams is not useful under low visibility (or in daylight), it should be tested as a possible alternative to currently used VASI systems which are generally useful only under good visibility conditions. The visual cues to the pilot are likely to be more reliable with the Glissada system than with the VASI, whose red beams can be lost leaving only the white beams.

The use of crossing light beams to mark the glide path appears to offer two advantages over current lighting systems. They give a positive indication of altitude, and they can be acquired sooner than the approach lights under low visibility conditions. The acquisition distance at the decision height for approach lights is usually 1600 ft [11]. Since the approach lights are 2-1/2 times brighter than the runway lights, they can be seen somewhat farther than the runway lights. For uniform visibility an RVR of 1400 ft should allow the approach lights to be acquired at 1600 ft. Since the night acquisition RVR for the crossed beams is 700 ft for 300-foot viewing, the crossed beam system is roughly twice as penetrating as the approach lights. The major uncertainty of the crossed beam system is the subjective response of the pilots to such lights. The system would work poorly during daytime and would probably not be feasible during the brightest daytime conditions ($B_o=10^4$ cd/m^2). Another interesting feature of the crossed beam system is that it offers some help for the SVR (Slant Visual Range) problem of telling the pilot when he can expect to acquire the ground. The beams crossing at the decision height could probably be seen by the pilot if the beam crossing could be seen by ground observers at a similar distance.

A visible laser guidance system has been shown to be feasible for certain system configurations and visibility conditions. Based on these, the following specific tasks are recommended to further the development of this technique.

1. Install a two-beam Glissada type system at a small airport and directly compare it with a VASI.
2. Install a two-beam system crossing at the decision height to provide location, altitude, and, possibly slant range information.
3. Simulate on computer the real-time signatures seen by a pilot viewing a multiple-crossed beam system. (Software changes could then be used to find out the effects of beam spacing, angle, width, etc.)

APPENDIX A. EYE/THRESHOLD MODEL

This appendix combines the results of two papers (Lamar, et al. [7] and Blackwell [10]) to obtain a model for the eye's detection of line sources. The Lamar report made measurements of the eye's response to rectangular light sources. It found that the eye responds to an angular width $\Delta\theta/2$ around the perimeter of such sources where the value of $\Delta\theta$ depends upon the background luminance. Unfortunately, Lamar considered only two levels of luminance. In this appendix the concepts of the Lamar study are used to interpret Blackwell's data on circular sources in order to derive an eye model which can be used at any practical value of background luminance (B_o).

Blackwell's data are plotted in Figure A-1 in the form used by Lamar. The light flux (contrast threshold $\Delta I/I$ times angular area) is plotted against the perimeter of the source for six values of background luminance. For small perimeters the eye simply responds to the total light flux from an effective point source. Beyond a certain perimeter the threshold flux increases because the center of the source disk is ineffective in exciting the eye. The Lamar model has the form

$$\Delta I/I \; A_u = cp^k \quad d>\Delta\theta \quad , \tag{A1}$$

where $p = \pi d$ is the source perimeter, d is the disk diameter, k is an exponent, c is a constant, and Au is the useful area given by

$$A_u = \frac{\pi}{4} \left[d^2 - (d-\Delta\theta)^2 \right] \quad . \tag{A2}$$

The data in Figure A-1 can be related to equation (A1) by $(\Delta I/I)A = (\Delta I/I)A_u(A/A_u)$. The resulting expression becomes

$$(\Delta I/I) \; A = C\pi^k \; d^{k+2} / \Delta\theta(2d-\Delta\theta). \tag{A3}$$

For $d \leq \Delta\theta$ we obtain

$$(\Delta I/I) \; A = C\pi^k \; \Delta\theta^k \quad . \tag{A4}$$

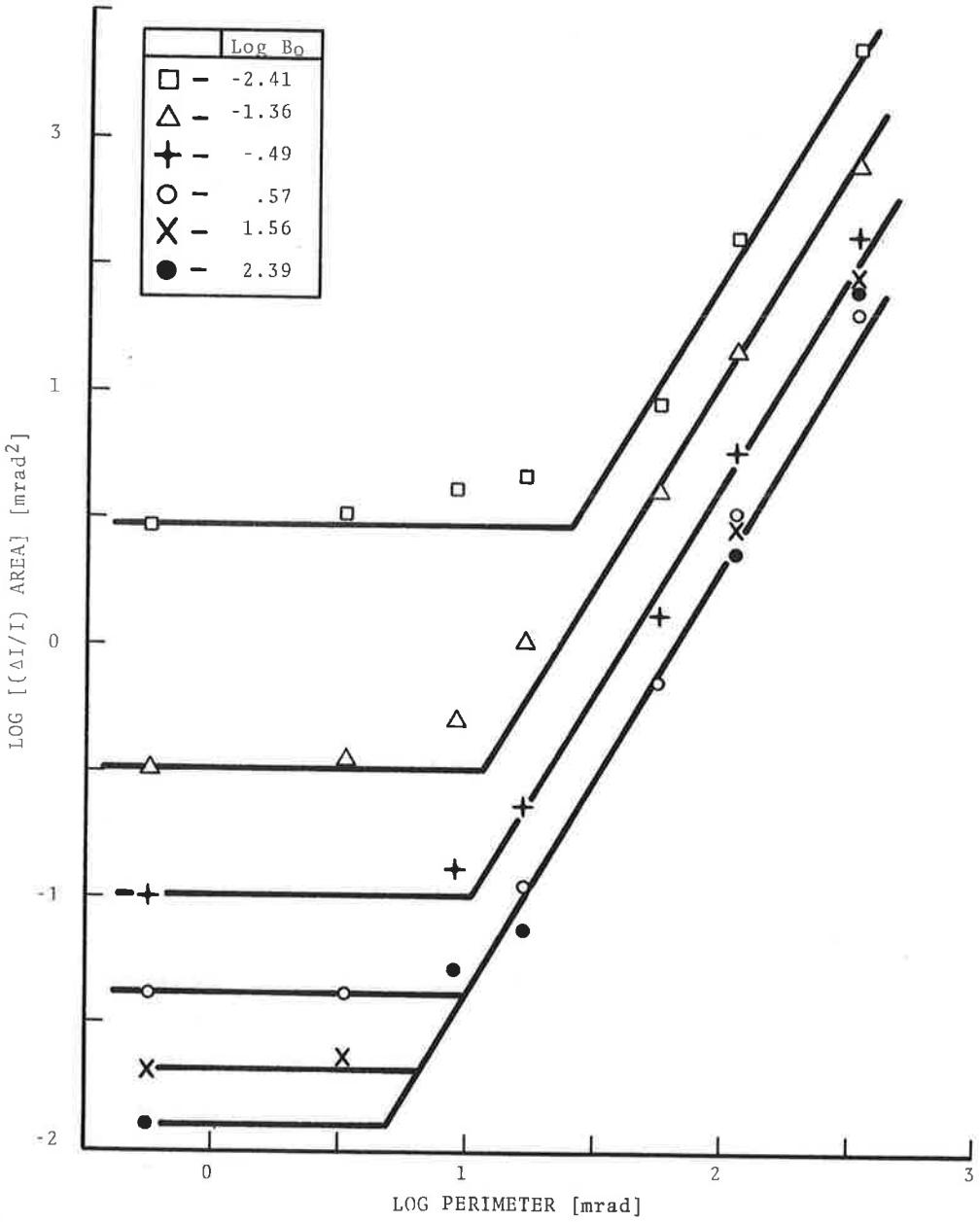

FIGURE A-1. CONTRAST THRESHOLD VERSUS SOURCE PERIMETER

For d >> $\Delta\theta$ we obtain the approximate result

$$(\Delta I/I)\ A = \frac{1}{2}\, c\pi^k \quad \frac{d^{k+1}}{\Delta\theta} \quad . \tag{A5}$$

The log-log slope is k+1. The data in Figure A-1 give a reasonable fit to the value k = 3/4, which Lamar found for the highest value of background luminance. The intercept d_i of the line with slope k+1 (Eq. A5) with the constant value (Eq. A4) can be used to determine $\Delta\theta$ from the data. Equating (A4) and (A5) gives

$$\log\ (\Delta\theta/d_i) = -\ (\log\ 2)/(k+1) \quad . \tag{A6}$$

These intercepts were used to obtain the values for $\Delta\theta$ plotted in Figure 2 as circles. The Lamar values are plotted as crosses. The straight line will be used to fit the data. The point-source threshold luminance B_t times the angular area is plotted in Figure A-2 for both the data from Figure A-1 (circles) and that from Lamar (crosses). The differences between the two are partly accounted for by the fact that Lamar uses a 5/8 detection probability while Blackwell uses a 1/2 detection probability. Presumably the rest of the discrepancy has to do with differences in the experiments. Threshold values obtained from correlating the Blackwell data with the Lamar data are used to derive the model for line detection.

We now recast equation (A1) in a form convenient for viewing line sources. Let us assume that the angular length L of the line source is much greater than the width W. The useful area (A_u) is then $L \cdot W_{eff}$ where $W_{eff}=W$ for $W \leq \Delta\theta$ and $W_{eff}=\Delta\theta$ for $W \geq \Delta\theta$. The perimeter is 2L. The threshold value holds for $L<\Delta\theta$:

$$B_t\ W_{eff} = (BA)_t\ /\ L \quad . \tag{A7}$$

At $L=\Delta\theta$ one obtains

$$B_t\ W_{eff} = (BA)_{t/\Delta\theta} \quad . \tag{A8}$$

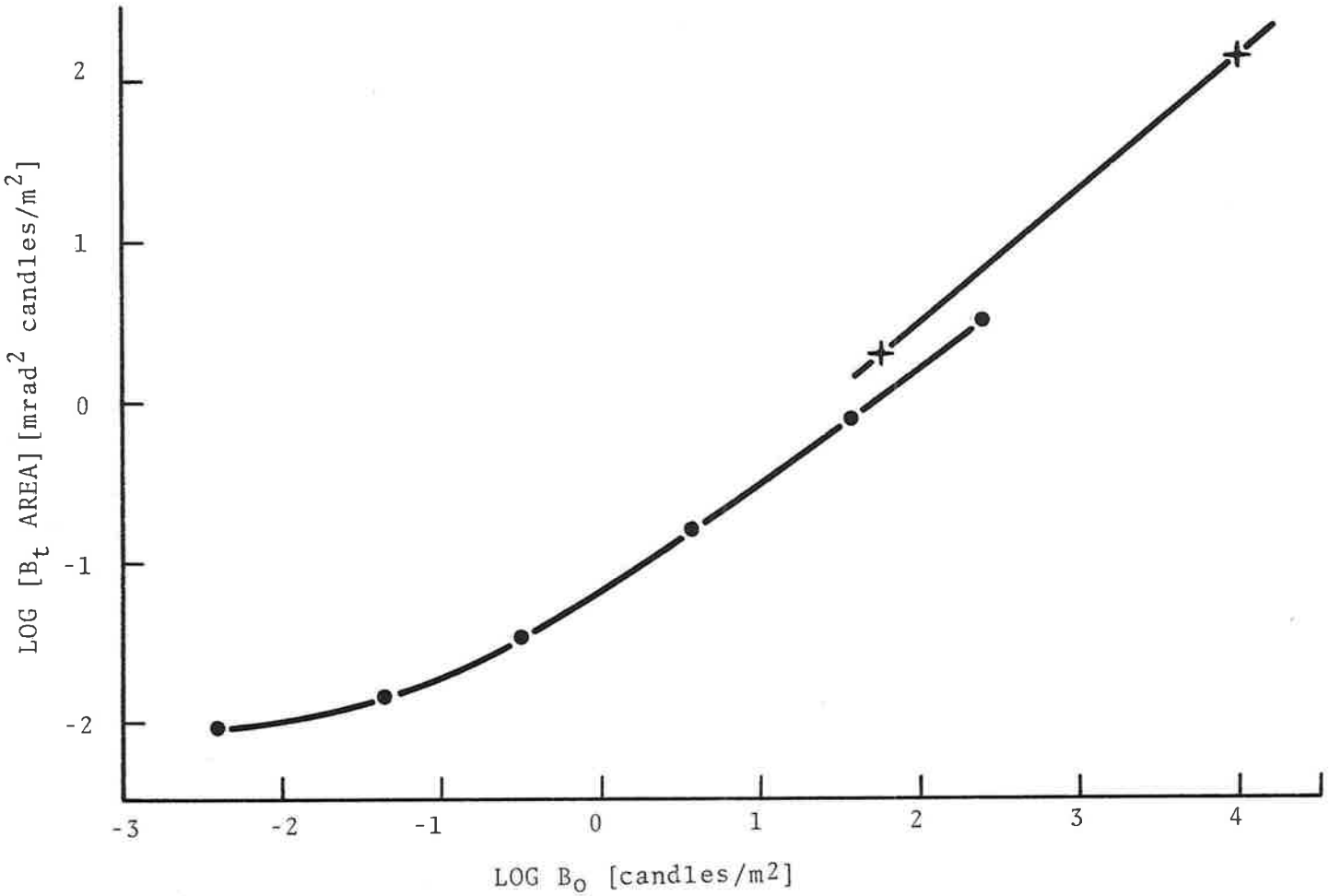

FIGURE A-2. POINT SOURCE THRESHOLD LUMINANCE TIMES THE ANGULAR SOURCE AREA VERSUS THE BACKGROUND

For $L>\Delta\theta$ one has an L dependence according to equation (A1),

$$B_t W_{eff} = (BA)_t (L/\Delta\theta)^{k-1}/\Delta\theta \ . \qquad (A9)$$

The parameters $\Delta\theta$ and $(BA)_t$ can be obtained, respectively, from Figures 2 and A-2. The curves for four values of B_o are shown in Figure 3. The point where $L=\Delta\theta$ is plotted from equation (A8) and the slopes -1 and $k-1 = -1/4$ are used for $L<\Delta\theta$ and $L>\Delta\theta$ on the log-log plot.

APPENDIX B. COMPARISON OF LASERS AND CONVENTIONAL LIGHT SOURCES

As far as visual perception is concerned, lasers and conventional light sources can be compared directly by considering only a small number of parameters. The basic parameters of a beam are its diameter, its angular divergence, and its luminous intensity. The associated cost parameters of size, power consumption, and capital and operating expenses are directly involved in the relative merits of lasers and conventional light sources. The optimum light source depends upon the system requirements. Lasers have extremely high brightness but low efficiency. They are best when sharp, narrow beams at long range are required. The higher efficiency of conventional light sources will cause them to be favored when broader beams are required.

Consider the luminous efficiency of various light sources. Lasers have very low efficiency in terms of optical power out divided by electrical power in. Typical values for CW visible lasers are 0.1 percent for He-Ne lasers and 0.01 percent for Ar^+ lasers. The luminous efficiency in terms of lumens per optical watt is high (673 lm/W maximum at 555 nm): 150 lm/W for the red He-Ne laser and 500 lm/W for the green Ar^+ laser. Combining these two efficiencies leads to a total luminous efficiency of 0.15 lm/W and 0.05 lm/W for He-Ne and Ar^+ lasers, respectively. The luminous efficiency of high pressure arc lamps is in a range of 20 to 30 lm/W and of tungsten-halogen lamps, 20 lm/W.

The spot size of a light beam at a distance is governed by the diameter of the collimating lens or mirror and by the intrinsic size of the light source. A single-mode laser has an intrinsic source size of one wavelength. It is completely coherent and therefore requires a minimum collimating optic diameter to produce a given beam divergence. (Note, however, that eye safety considerations may require larger optics.)

A conventional light source may require inordinately large diameter optics to produce an acceptable beam divergence for a

particular system. The beam divergence is given by $\Delta\theta = d/F$, where d is the width of the light source and F is the mirror focal length. Results of a comparison of five different light sources are shown in Table B-1.

One must beware of blind comparisons between these numbers. The narrow laser beam divergences result in no beam spreading for these laser beams over the ranges of interest (<10 km). The numbers for the searchlight and the signal light do not include the large amount of light outside the main beam, which could interfere with operations of a system and therefore might require additional beam shaping optics.

Another way of comparing laser sources with conventional ones is to calculate the divergence angle required to reduce the luminous intensity to that of the L.S.5 runway lights (10,000 cd). A He-Ne 50 mW laser has this luminous intensity for a solid angle of 4.5×10^{-4} sr (0.024 radian cylindrical beam width). The corresponding angles for a 2 W Ar^{+} laser are 10^{-1} sr and 0.36 rad.

Consider the two types of systems discussed in Section 7.2. The first requires narrow beams to be generated at runway threshold and projected to the middle marker (about 1000 m away). If such a beam must remain less than 2 m in diameter, the divergence of 0.002 rad is probably too small to be obtained from a searchlight and a laser would be preferred. However, if one wanted to illuminate the portion of the approach path where the pilot is likely to be (30 m diameter circle) an angular divergence of 0.03 rad could be easily obtained with a search light. As a third case, consider a beam intersecting the glide slope of the middle marker (about 60 m altitude). If the beam diameter must be 2 m and the range is 100 m, the 0.02 radian divergence can also be obtained from a searchlight. The fifth source in Table A-1 would be satisfactory since the beam must be narrow in only one direction.

One last consideration is the possible advantage the marked color of a laser may present as a contrast to the white background luminance of the sky. One can change a white light to green.

If a uniform spectral source is passed through a green band pass filter between 495 nm and 565 nm wavelength, the loss in luminous intensity is only 50 percent.

TABLE B-1. LIGHT SOURCE CHARACTERISTICS

SOURCE	BEAM DIVERGENCE (RADIANS)	PEAK CANDLE POWER (CANDLES)	LUMINOUS FLUX WITHIN DIVERGENCE ANGLE (LUMENS)	ELECTRICAL POWER (WATTS)	EST. COST (DOLLARS)
50 mW He-Ne Laser (30 cm Optics)	5.1×10^{-6}	2.2×10^{11}	4.5	50	8,300
2W, Ar^{+} Laser (30 cm Optics)	4.2×10^{-6}	7.2×10^{13}	1000	10^{4}	9,995
Arc, Searchlight (75 cm Optics)	2.3×10^{-2}	2.5×10^{7}	≃4000	4.5×10^{3}	12,000
Arc, Signal Light (75 cm Optics)	3.5×10^{-2}	1.5×10^{6}	—	10^{3}	2,000
100W, Tungsten-Halogen (Rectangular 30 cm Optics)	1.9×10^{-2} x 6.4×10^{-2}	1.2×10^{6}	1500	100	500

REFERENCES

1. Basov, N.G., et al., "Aircraft Take-Off and Landing System and Method for Using Same," U.S. Patent No. 4,063,218 (13 December 1977).

2. Viezee, W., J. Oblanas, and M. Glaser, "Feasibility of Laser Systems for Aircraft Landing Operations Under Low Visibility Conditions," U.S. Department of Transportation, Federal Aviation Administration, Washington DC (October 1974), FAA-RD-74-190.

3. Lawson, A.J., J.K. Marut, and R.L. Northedge, "Tables of Runway Visual Range Values As A Function of Transmittance and Various Values of Pilot's Illuminance Threshold and Light Targets," U.S. Department of Transportation, Federal Aviation Administration, Washington DC (August 1970).

4. Middleton, W.E. Knowles, Vision Through The Atmosphere, University of Toronto Press, Ontario, Canada (1952), p. 97.

5. _____, p. 12-17.

6. _____, p. 48.

7. Lamar, E.S., et al., "Size, Shape, and Contrast in Detection of Targets By Daylight Vision. Volume I: Data and Analytical Description," J. Opt. Soc. Am. 37, 7 (1947).

8. Edelberg, S., "An Overview of the Limitations on the Transmission of High Energy Laser Beams Through the Atmosphere by Nonlinear Effects," Advisory Group for Aerospace Research and Development Conference Proceedings, No. 183, Neuilly Sur Seine, France (October 1975).

9. "Performance Standard for Laser Products," Bureau of Radiological Health; U.S. Department of Health, Education, and Welfare; Federal Register 40, 148 (31 July 1975).

10. Blackwell, H.R., "Contrast Thresholds of the Human Eye," J. Opt. Soc. Am. 36, 624 (1946).

11. "Visual Guidance Lighting Systems," Handbook 6850.2, U.S. Department of Transportation, Federal Aviation Administration, Washington DC (29 May 1962).

BIBLIOGRAPHY

"Basic Flight Information and ATC Procedures," Airman's Information Manual, U.S. Department of Transportation, Federal Aviation Administration, Washington DC (January 1977), AIR/GEN/SAR/RAC/COM 1/AGA 3, I.

Bradley, G.S., C.W. Lohkamp, and R.W. Williams, "Flight Test Evaluation of Slant Range Visual Range/Approach Light Contact Height (SVR/ALCH) Measurement System," U.S. Department of Transportation, Federal Aviation Administration, Washington DC, FAA-RD-76-167 (November 1976).

Chu, T.S. and D.C. Hogg, "Effects of Precipitation on Propagation At 0.63, 3.5, and 10.6 Microns," Bell System Technical Journal 47, 5 (May - June 1968).

Gebhardt, F.G., "Self-Induced Thermal Distortion Effects on Target Image Quality," Applied Optics 2, 6 (June 1972).

Hogge, C.B., "Atmospheric Effects on High Energy Laser Beams," In: Proceedings of Third American Meteorological Society Conference on Atmospheric Radiation, Davis CA (28-30 June 1978).

Ingrao, H.C., et al., "The Development of A Signal Data Converter for an Airport Visibility Measuring System," U.S. Department of Transportation, Federal Aviation Administration, Washington DC, FAA-RD-75-65 (August 1975).

Klass, P.J., "Soviet Landing Aid Draws FAA Security," Aviation Week and Space Technology 108, 42 (12 June 1978).

Larsson, A.J., J.K. Marut, and R.L. Northedge, "Tables of Runway Visual Range Values as a Function of Transmittance and Various Values of Pilot's Illuminance Threshold and Light Targets," U.S. Department of Transportation, Federal Aviation Administration, Washington DC, FAA-RD-70-58, (August 1970).

Lifsitz, J.R., "The Measurements of Atmospheric Visibility with Lidar: TSC Field Test Results," U.S. Department of Transportation, Federal Aviation Administration, Washington DC, FAA-RD-74-29 (March 1974).

Mason, J.B. and J.D. Lindberg, "Laser Beam Behavior on a Long High Path," Applied Optics 12, 2 (February 1973).

BIBLIOGRAPHY (CONT.)

"Pilots Cautioned on the Use of VASI Below 200 Feet," Monthly Aviation Wrap-Up 6, 11 (November 1978).

Rockwell, R.J., Jr., D.H.. Sliney, and J.F. Smith, "Laser Safety, Part I: Introduction to Hazard Calculations," Electro-Optical Systems Design 10, 25 (November 1978).

"Site Requirements For Terminal Navigational Facilities," Airport Design STandards, U.S. Department of Transportation, Federal Aviation Administration (21 September 1973).

Viezee, W., E.E. Uthe, and R.T.H. Collis, "Lidar Observations of Airfield Approach Conditions: An Exploratory Study," Journal of Applied Meteorology 8, 274 (April 1969).

Wyman, P.W., "Laser Radar Eye Hazard Considerations," Applied Optics 8, 2 (February 1969).

220 copies

U.S. DEPARTMENT OF TRANSPORTATION
RESEARCH AND SPECIAL PROGRAMS ADMINISTRATION
TRANSPORTATION SYSTEMS CENTER
KENDALL SQUARE, CAMBRIDGE, MA. 02142

OFFICIAL BUSINESS
PENALTY FOR PRIVATE USE, $300

POSTAGE AND FEES PAID
U.S. DEPARTMENT OF TRANSPORTATION
513